Title: Differentially phased leaf growth and movements in Arabidopsis depend on coordinated circadian and light regulation.
Authors: Dornbusch T, Michaud O, Xenarios I, Fankhauser C
Journal: The Plant cell
Year: 2014 Oct
Volume: 26
Issue: 10
Pages: 3911-21
DOI: 10.1105/tpc.114.129031

Title page.

Differentially phased leaf growth and movements depend on coordinated circadian and light regulation.

Tino Dornbusch[1], Olivier Michaud[1], Ioannis Xenarios[2] and Christian Fankhauser[1, 3]

[1] Center for Integrative Genomics, Faculty of Biology and Medicine, University of Lausanne, 1015 Lausanne, Switzerland

[2] SIB-Swiss Institute of Bioinformatics, University of Lausanne, 1015 Lausanne, Switzerland

[3] Author for correspondence: christian.fankhauser@unil.ch

Keywords: leaf growth, leaf movements (hyponasty), circadian clock, EARLY FLOWERING 3 (ELF3), PHYTOCHROME INTERACTING FACTOR (PIF), laser scanning.

Short title: Coordination of leaf growth and movements

Abstract

In contrast to vastly studied hypocotyl growth, little is known about diel regulation of leaf growth and its coordination with movements such as changes in leaf elevation angle (hyponasty). We developed a 3D live leaf growth analysis system enabling simultaneous monitoring of growth and movements. Leaf growth is maximal several hours after dawn, requires light and is controlled by day length suggesting coupling between growth and metabolism. We identify both, blade and petiole positioning as important components of leaf movements and reveal a temporal delay between growth and movements. In hypocotyls the combination of circadian expression of *PHYTOCHROME INTERACTING FACTORS 4* and *5* (*PIF4* and *PIF5*) and their light-regulated protein stability drives rhythmic hypocotyl elongation with peak growth at dawn. We find that PIF4 and PIF5 are not essential to sustain rhythmic leaf growth but control their amplitude. Furthermore, EARLY FLOWERING 3 (ELF3), a member of the evening complex (EC), is required to maintain the correct phase between growth and movement. Our study shows that the mechanism underlying rhythmic hypocotyl and leaf growth differ. Moreover, we reveal the temporal relationship between leaf elongation and movements and demonstrate the importance of the EC for the coordination of these phenotypic traits.

Introduction

The survival of most organisms on earth depends on plants using solar energy, water, nutrients and CO_2 to fuel their own growth. The conversion of solar into chemical energy happens primarily in leaves, but surprisingly little is known about the regulation of growth of leaves themselves. It has been shown that growth of leaves and other plant structures occurs with a diel (24 hour) rhythm (Nozue et al., 2007; Wiese et al., 2007; Yazdanbakhsh et al., 2011; Farre, 2012; Ruts et al., 2012a), which is not entirely surprising given that the ever-occurring day-night alternations profoundly affect plant metabolic reactions. The circadian clock and leaf starch metabolism regulate the growth patterns of roots and leaves (Wiese et al., 2007; Yazdanbakhsh et al., 2011; Ruts et al., 2012b). However, detailed kinetics of diel leaf growth rhythms - a prerequisite to understand the molecular mechanisms underlying growth control - remain scarce (Wiese et al., 2007; Ruts et al., 2012b). This presumably results from leaf movements accompanying leaf growth and thereby complicating growth analysis in living plants (Wiese et al., 2007).

Growth rhythms are best understood in hypocotyls (one-dimensional) where they depend on a coordinated control by light, the availability of carbon and the circadian clock (Nozue et al., 2007; Nusinow et al., 2011; Stewart et al., 2011). In the presence of sufficient resources rhythmic hypocotyl growth peaks at the dark-light transition (dawn). This rhythm depends on an external coincidence mechanism whereby circadian expression of *PHYTOCHROME INTERACTING FACTOR 4* and *5* (*PIF4* and *PIF5*) and light-regulated degradation of these bHLH factors leads to their maximal activity around dawn (Nozue et al., 2007). Repression of *PIF4* and *PIF5* expression earlier in the night depends on the evening complex, which is composed of EARLY FLOWERING 3 and 4 (ELF3, ELF4) and LUX ARRHYTHMO (LUX) and prevents excessive growth earlier in the night (Nusinow et al., 2011).

Different types of movements accompany rhythmic leaf growth (Wiese et al., 2007; Whippo and Hangarter, 2009; Dornbusch et al., 2012). Diel leaf movements are a well-characterized output of the circadian clock (Farre, 2012). In addition, movements with much shorter periods known as circumnutations occur in many plant structures

including growing leaves (Stolarz, 2009; Whippo and Hangarter, 2009). All these movements are known to be associated with growth and/or reversible cell enlargement at the level of the petiole (the structure connecting the leaf blade to the stem). In some plant species such as *Mimosa pudica* specialized cells at the base of the petiole form the pulvinus that allows for rapid reversible changes in leaf position (Whippo and Hangarter, 2009). Plants like *Arabidopsis thaliana*, which do not possess such pulvini, also undergo leaf movements that at least partially depend on differential growth of the adaxial and abaxial sides of the petiole (Polko et al., 2012; Rauf et al., 2013). However, the coordination and relationship between leaf movements and growth remain largely unknown.

The movements accompanying rhythmic leaf growth render kinetic growth-analyses challenging prompting some authors to prevent leaf movements to measure growth (Wiese et al., 2007). Moreover, simultaneous analyses of leaf growth and movements have not been reported previously thereby making it difficult to understand the relationship between these phenomena. We used near infrared laser scanning and developed novel imaging algorithms allowing us to follow growth, nutations and movements of the same leaves with high spatial and temporal resolution. We found that leaves accelerate elongation growth several hours prior to upward movements of the leaves (leaf hyponasty). Proper phasing between elongation and hyponasty depends on ELF3 a member of the evening complex. As in hypocotyls, leaf growth rhythms in day-night conditions are coordinately regulated by the interplay between light and circadian signals. However, our results in leaves show that the underlying molecular mechanism differs from the one that was previously uncovered in the control of hypocotyl growth.

Results

Development of a method allowing simultaneous analysis of leaf growth and movements.

To analyze the relationship between leaf growth and movements, we developed an image analysis algorithm to measure single leaves using a previously described laser scanning method (Dornbusch et al., 2012). *Arabidopsis* plants were imaged at intervals of 10 or 60 minutes and time-lapse images were analyzed to track a point at the base (P_0), at the petiole-blade-junction (P_P) and at the tip (P_T) of each individual leaf (Figures 1A, B, Supplemental Figure 1; Supplemental Movie 1). The vector P_0P_T defines length l_{tip} and elevation angle Φ_{tip} of each leaf while the same traits for the petiole vector and blade vector are l_{pet}, Φ_{pet} and l_{bl}, Φ_{bl}, respectively (Supplemental Figure 2A). The leaf-tracking algorithm was validated comparing data from the laser scanning system with measurements on simultaneously photographed plants (Supplemental Movie 2). This analysis demonstrated the precision of our system (Figures 1C, D). Although l_{tip} is somewhat shorter than the precise leaf length (l_{leaf}, Supplemental Figure 2A), we showed that diel leaf elongation rate (integrated over 24h) and the growth rhythms were highly similar for both l_{tip} and l_{leaf} (Supplemental Figure 2B). Therefore, in the following we primarily used leaf elongation rate computed from l_{tip} to discuss the diurnal pattern of growth. For simplicity we refer to elongation rates as growth and changes in elevation angles as movements. When imaged at 10-minute intervals we can also measure ultradian circumnutations (nutations) that are distinct from the diurnal leaf movements (Supplemental Figure 2C).

Due to geometric constraints from the measuring device the entire leaf can be scanned with most precision in plants with relatively horizontal leaves. This dictated our choice to start our analysis in plants grown in long days (L/D, 16/8h) released into continuous days (L/L) where the leaf positions remain relatively horizontal. Both growth and movements followed a rhythmically oscillating pattern consistent with a circadian control of growth and movement (Figure 2, Supplemental Figure 2C, see below). By simultaneously analyzing growth rates and movements we observed that the phase of both peaks was distinct (Figure 2, Supplemental Figure 2C). Growth was

minimal during the subjective night around Zeitgeber Time 20 (ZT20) and peaked in the subjective morning around ZT3-4. Leaf elevation angle Φ_{tip} was minimal around ZT2 and reached a maximum in the subjective evening at ZT14 (Figure 2, Supplemental Figure 2C). In order to better compare the growth rate with movement, we also plotted the rate of change of leaf position (in $°h^{-1}$) (Figure 2C, 3A). This method allows comparing acceleration of growth (slope in Fig. 2A) with acceleration of up- and downward movement (slope in Fig. 2C). It confirms a phase difference of ~3h between acceleration of growth and movement (Figure 3A). Finally, we noticed that upward movement of leaves largely coincided with a phase of nutations that faded out around ZT16 when leaves started to move down (Supplemental Figure 2C).

Both petiole and blade contribute to the patterns of leaf growth and hyponasty

By analyzing leaf growth and movement we identified the temporal relationship between the phases of upwards movement and acceleration of growth (Figures 2, 3A). In order to uncover how blade and petiole contribute to these patterns we measured them separately. Our measurements revealed that at ZT20 the leaf blade started to elongate several hours before the petiole (Figure 3B, see arrows). This initial blade growth phase occurred at a time when both the petiole and the blade still moved down explaining why the leaf tip moved downwards around subjective dawn (Figure 2B). The leaf blade accelerated its movement around ZT0 (Fig. 3C) and moved upwards when it reached its maximal elongation rate (approximately ZT2), a time that also corresponded to an increase in petiole growth rate (Figure 3B). Petioles moved with similar amplitude as blades and accelerated their movement shortly after blades, but at a slower rate (Figure 3C). Similarly to the blades they started to move upwards when reaching their maximal growth rate (Figures 3B-D). Finally, we noticed that while blade growth showed one growth peak shortly after subjective dawn, the petiole showed a morning growth peak and a second one before subjective dusk (Figure 3B). These experiments indicate that around subjective dawn both growth and movement first start in the blade and then in the petiole. Moreover, in both parts of the leaf rapid upward movement starts significantly later than acceleration of growth (Figures 2, 3).

To determine whether leaf blade position also contributes to leaf hyponasty in other growth conditions we analyzed blade and petiole position in L/D-grown plants and in plants transferred into simulated shade which is known to enhance leaf hyponasty

(Moreno et al., 2009; Dornbusch et al., 2012). In both conditions blade movement clearly contributed to overall leaf hyponasty (Supplemental Figure 3 and 4). Moreover, both in L/D conditions and in response to simulated shade the blade started to move upwards prior to the petiole (Supplemental Figure 3 and 4, see arrows). Collectively these experiments identify the movement of the blade as an important contributor of leaf hyponasty and show that blade movement precedes petiole movements.

Changes in the light environment differentially affect leaf growth and movements.

Earlier studies in Arabidopsis have identified a differential growth response between the adaxial and abaxial sides of the petiole as a mechanism underlying leaf hyponasty (Polko et al., 2012; Rauf et al., 2013). This suggests that Arabidopsis leaf hyponasty is primarily a growth driven process. Our work shows that there is a temporal shift between growth and movement (Figures 2, 3, Supplemental Figure 3 and 4), suggesting a more complex relationship between these two processes. In order to test this further we analyzed growth and movement in plants grown in different light regimes and plotted diel (24h) growth rates and diel leaf movements (Figure 4). This comparison showed that a decrease in PAR (Photosynthetically Active Radiation) and a decrease in daylength alter the relationship between growth and movements. In short-day conditions (S/D) diel leaf growth rate was decreased, whereas the magnitude of diel movements was similar in S/D compared to L/L or L/D (Figure 4). Low PAR-grown plants also showed decreased growth, but increased diel leaf movements compared to L/L or L/D (Figure 4) consistent with other finding of low-PAR-induced hyponasty (Keller et al., 2011). These experiments suggest a partial uncoupling between the magnitude of growth and movement.

Light is required to initiate leaf growth at dawn

Rhythmic growth of hypocotyls is controlled by a combination of circadian and light cues (Nozue et al., 2007); we thus compared leaf growth and movements between plants maintained in day-night and plants released into constant light (L/L). In L/D, growth was minimal at dawn several hours later than in LL (ZT20 in L/L, ZT0 in L/D) (Figure 5A, see arrows). In long-day-grown plants the increase of the growth rate coincided with lights on but the timing of the morning peak was similar in L/D and L/L (Figure 5A). In L/D the second growth peak preceding dusk at ZT16 was

more pronounced in L/D than L/L (Figure 5A). The diurnal pattern of leaf elevation angle was similar in L/D and L/L. Minimum values for Φ_{tip} were observed at the time of the morning growth peak at ZT3 and maximum values around ZT13-14 (Figure 5B). Hence, similar phasing between growth and movements was maintained in both conditions (Figure 5B). In our growth chamber light-dark transitions are abrupt. At dusk this coincided with a transient upward movement (strong acceleration of movement) (Figure 5B, C). Downward movement accelerates in the second half of the night followed by a brief reacceleration of first downward then upwards movement at dawn (Figure 5C). Our data thus show that the circadian clock controls both movement and growth rhythms and that day-night transitions influence these patterns.

When grown in day-night conditions, the leaf growth rate was at its minimum at the end of the night (ZT0) and rapidly increased after dawn (Figure 5). In order to test whether light is essential to induce growth in the morning, we entrained plants in L/D (16/8h) and imaged them prolonging the night for 3 hours before dusk ($L/_{+3}D$) or after dawn (L/D_{+3}). At L/D_{+3}, leaves did not start growing at ZT0 but at actual dawn ZT3 (Figure 6A). At $L/_{+3}D$, the first growth peak remained at ZT0, but the second growth peak was shifted to ZT13 (Figure 6B). These experiments show that in sharp contrast to the situation hypocotyls where light inhibits growth at dawn (Nozue et al., 2007), the induction of leaf growth at dawn requires light (Figures 5, 6). The growth pattern in L/L suggests that the effect of light to trigger growth is gated by the circadian clock (Figure 5). In order to test this further we switched on the light 3 hours earlier in L/D-grown plants (L/D_{-3}). Our experiment showed that in those conditions light was not sufficient to trigger rapid leaf elongation, which did not start much before ZT0 (Supplemental Figure 5C). Collectively, these experiments show that both the circadian clock and light shape leaf growth rhythms and show that light is essential at dawn to initiate growth (Figures 5, 6).

The need for light at dawn to initiate leaf growth could result from the need for photosynthates. We decided to indirectly test this idea by growing plants in different light regimes. Plants partition more resources into starch when grown in short days (S/D) than in long days suggesting that they may have more resources available to fuel growth early in the morning when grown in L/D (Stitt and Zeeman, 2012; Sulpice

et al., 2013). We therefore compared growth and movements in S/D and L/D-grown plants and found that in both conditions growth in the morning required light and that the morning growth-peak was reduced in S/D compared to L/D (Supplemental Figure 6). In contrast to L/D conditions, we could not detect a second growth peak preceding dusk (ZT8), but rather a peak during the night at ZT12 (Supplemental Figure 6). Overall growth was reduced in S/D-grown plants but more growth (in relative terms) occurred at night in S/D-grown plants than in L/D plants (Supplemental Figure 6). As S/D-grown plants invest more resources into starch this finding is compatible with a metabolic role of light in the control of growth patterns (Stitt and Zeeman, 2012; Sulpice et al., 2013). In contrast to diel growth rates, day length moderately affected the pattern and the magnitude of diel leaf movements, except that dusk altered leaf position in L/D but not in S/D (Figure 4, Supplemental Figure 6).

Our results suggest that light-induced metabolism is required to promote leaf growth. To test this further we compared growth of L/D-grown plants in either in high or low PAR and found that in low PAR the magnitude of leaf growth was reduced (Figure 4). We also transferred L/D-grown plants into D/D, which lead to a decrease in the diel growth rate (Figure 4)**.** Consistent with our night extension experiment (Figure 6A), there was no growth induction shortly after subjective dawn in D/D (Supplemental Figure 6B), however there was a transient growth peak around ZT6-8 (Supplemental Figure 6B). Upon return into the light the leaf growth rate increased rapidly (Supplemental Figure 6B, black arrow). Taken together our results are consistent with a metabolic role of light to initiate leaf growth at dawn (Figures 4, 5, 6, Supplemental Figures 5, 6).

The phase relationship between leaf growth and movements requires a functional evening complex.

Our results show that day-night cycles interplaying with the circadian clock orchestrate the diurnal patterns of growth and movement. Rhythmic hypocotyl growth is also coordinately controlled by the circadian clock and light cues that converge on the regulation of PIF4 and PIF5 (Nozue et al., 2007). We thus analyzed leaf growth and movements of *pif4pif5* double mutants and found that, when grown in long days, this mutant displayed low amplitude growth and movement rhythms that were otherwise similar to those of the wild type (Figure 7A). Over-expression of PIF4 or

PIF5 and photoreceptor mutants cause a reduction of the amplitude in hypocotyl growth rhythms (Nozue et al., 2007). The situation was different for leaf growth as PIF4 over-expression and *phyB* mutants maintained robust leaf growth rhythms although in these mutant backgrounds there was more leaf growth towards the end of the day (Supplemental Figure 7). High PIF4 and PIF5 activity is prevented early in the night by the evening complex that restricts the expression of *PIF4* and *PIF5* and hypocotyl growth during the night (Nozue et al., 2007; Nusinow et al., 2011). To investigate the role of the evening complex in rhythmic leaf growth we analyzed the *elf3* mutant. When grown in long days, *elf3* displayed its major growth peak at the end of the night indicating that the evening complex prevents leaf growth at night (Figure 7B, see arrows) (Nozue et al., 2007). In addition, maximal growth rates in the *elf3* mutant coincided with maximal leaf angles, showing that ELF3 is needed to maintain the normal phase relationship between leaf growth and movement (Figure 7B, see arrows). Analysis of *elf3* and *pif4pif5* grown in constant light confirmed the importance of the circadian clock for rhythmic growth and movements and revealed a moderate phase phenotype in *pif4pif5* (Figures 7C, D). Collectively, our data show that the mechanism controlling rhythmic growth in leaves and hypocotyls differ and reveal that ELF3 is required for normal phasing between leaf growth and movements.

Discussion

Live measurements of leaf growth and/or leaf movements have been reported before (Wiese et al., 2007; Walter et al., 2009; Bours et al., 2012), however our method is unique in that it simultaneously but separately reports on both growth and movements (Figure 2, Supplemental Figure 2). By imaging at sufficient frequency (every ten minutes rather than hourly) we reduce the number of plants that we can simultaneously analyze but this enables us to characterize circumnutations (Supplemental Figure 2C). Future work should allow us to better understand the mechanisms underlying this well-known form of "rapid" plant movements that has been discussed since the times of Charles Darwin but remain poorly understood (Whippo and Hangarter, 2009). The geometry of the laser scanning system is well suited for relatively flat and horizontally oriented objects like an Arabidopsis rosette. Imaging the entire leaf, in particular the blade-petiole junction becomes difficult when leaves are erect which is why we use l_{tip} rather than l_{leaf} (Supplemental Figure 2A). Importantly, our data show that l_{tip} is an excellent proxy to determine leaf elongation rates (Supplemental Figure 2B). Moreover, our data correlates well with relative leaf surface growth rhythms (our own observations) and with previous publications (Wiese et al., 2007; Walter et al., 2009; Ruts et al., 2012b). Although in these previous reports Arabidopsis rosettes where grown in 12/12 cycles, they also identified growth peaks early in the morning and towards the end of the day similar to our data in long days (16/8) (Figure 5) (Wiese et al., 2007; Ruts et al., 2012b).

By simultaneously tracking leaf movements and growth we determined that elongation growth precedes upward movement of the leaf (Figures 2, 3, 5, Supplemental Figures 5, 6). This is true when analyzed at the level of the entire leaf, the blade and the petiole (Figure 3). We thus conclude that a change in leaf hyponasty is the result of differential petiole growth as determined before (Polko et al., 2012; Rauf et al., 2013), but in addition blade growth and elevation angle (relative to the petiole) also contributes to the overall leaf position (Figure 3). We demonstrate the importance of leaf blade position in leaf hyponasty in several growth conditions (L/L, L/D and simulated shade) suggesting that this is a general feature of the leaf hyponasty response (Figure 3, Supplemental Figures 3, 4). In all cases analyzed

upward movements were initiated as the leaf (or part of it) reached its maximal elongation rate (Figures 3, 5, Supplemental Figures 5, 6), demonstrating a correlation between both processes (although with temporal delays). This finding is consistent with the fact that as leaves age both growth and movements decline (Mullen et al., 2006). However, our work also reveals that coupling between growth and movements is a regulated process as environmental stimuli differentially affect growth and movements (Figure 4). For example, when PAR is diminished, the leaf growth rate declines but the leaf movements increase (Figure 4). Moreover, in the *elf3* mutant, the phase relationship between the peak of growth and elevation angle was strongly altered (Figure 7B). Growth of different parts of the blade and petiole may contribute differentially to overall growth and changes in elevation angle and thereby explain the complex relationship between growth and movement reported here (Figure 3) (Wiese et al., 2007; Andriankaja et al., 2012; Polko et al., 2012; Remmler and Rolland-Lagan, 2012). In addition, reversible turgor pressure driven changes in cell size may also contribute to changes in leaf hyponasty (Mullen et al., 2006; Barillot et al., 2010).

By separately analyzing growth and movement of blades and petioles we observed that blades started to grow and move upwards 2-3 hours before the petiole (Figure 3). One possibility is that this is regulated by the combined action of auxin and carbohydrates (Lilley et al., 2012). Interestingly, rhythms in auxin responsiveness and soluble carbohydrates correlate quite well (Covington and Harmer, 2007). As the leaf blade is considered as a major source of auxin production (Tao et al., 2008), we propose that blade growth occurs before petiole growth because auxin first needs to be transported to the petiole. Interestingly, in L/L conditions a second growth peak occurred in petioles that we did not observe in the blade (Figure 3) indicating that the growth pattern is more complex in the petiole than the blade. Based on the analysis of overall leaf growth we can also conclude that these patterns are environmentally controlled (Figure 4). To fully understand the relationship between growth and movements our organ-level analysis needs to be combined with the determination of growth patterns with cellular resolution, which is very challenging at the level of expanded leaves (Ichihashi et al., 2011; Andriankaja et al., 2012; Polko et al., 2012).

By moving plants into constant darkness and performing night extension experiments we showed the requirement for light to initiate growth at dawn (Fig. 2, 3, 5). The light

effect around subjective dawn is gated by the circadian clock as shown by growing plants in L/L and by shortening the night in L/D plants (Figures 5, 6 and Supplemental Figure 5). Importantly, when the night is extended by 3 hours before the dark phase, the timing of the morning growth-peak was unaffected (Figure 6B). In contrast, extending the night by 3 hours in the morning delayed the acceleration of growth until the actual onset of light (Figure 6A). Plants precisely control starch degradation during the night and almost completely exhaust their reserves by dawn (Stitt and Zeeman, 2012). Starch metabolism is immediately adjusted if the night is extended due to an early onset but not if the night is extended beyond the subjective dawn. Moreover, exhaustion of starch resources at the end of the night limits Arabidopsis growth (Graf et al., 2010). These data together with our results suggest that light at dawn fuels leaf growth if growth repression by the circadian clock is released (Figures 5, 6, Supplemental Figure 5). Short-day grown plants accumulate more starch during the day in order to have enough resources at night. In such conditions, fewer resources will be immediately available for growth in the morning (Stitt and Zeeman, 2012). Consistent with this idea, our data show that the morning growth peak in short-day grown plants is reduced compared to long-day grown plants (Supplemental Figure 6A). Also consistent with this metabolic model is the relatively enhanced growth at night in short-day plants (Supplemental Figure 6A) (Sulpice et al., 2013), reduced growth in low PAR conditions (Figure 4) and the fact that starchless mutants invest more resources in growth during the day when solar energy is present (Wiese et al., 2007). It was recently reported that a long-term consequence of sugar starvation is a reduction of gibberellin synthesis that limits growth (Paparelli et al., 2013). However, it is unlikely that this gibberellin response can explain the immediate effect of light on growth in the morning reported here (Figures 5, 6). Finally, we wish to point out that when wild-type plants are kept in darkness for extended periods of time a short pulse of growth occurs about 6-8 hours after subjective dawn (Supplemental Figure 6B). This experiment indicates that alternative metabolic pathways (e.g. induction of autophagy) can be activated to fuel growth under exceptional circumstances (Usadel et al., 2008; Suttangkakul et al., 2011; Izumi et al., 2013).

ELF3 controls rhythmic growth of leaves, hypocotyls and roots (Figure 7) (Nozue et al., 2007; Nusinow et al., 2011; Yazdanbakhsh et al., 2011). Our work identifies

similarities and differences for ELF3 function in these different organs. In all organs, growth at night is restricted by ELF3 (Figure 7B, D) (Nozue et al., 2007; Nusinow et al., 2011; Yazdanbakhsh et al., 2011). The leaf growth peak towards the end of the night in *elf3* is surprising given that in the wild type light in the morning is essential to trigger growth (Figure 5A). A possible explanation for this observation is the incomplete starch degradation during the night in *elf3* (Yazdanbakhsh et al., 2011). This may explain how this mutant has sufficient resources at the end of the night to enhance leaf growth without the need for light (Figure 7). Interestingly long-day grown *elf3* mutants have reduced leaf growth, contrasting with enhanced rates of root and hypocotyl growth in this mutant (Figure 7) (Nozue et al., 2007; Nusinow et al., 2011; Yazdanbakhsh et al., 2011). These organ-specific effects on growth might be due to different partitioning of resources in *elf3* (Yazdanbakhsh et al., 2011).

In hypocotyls, the circadian expression of *PIF4* and *PIF5* in conjunction with light-induced PIF4 and PIF5 protein degradation explains a rhythmic growth pattern with a major peak at dawn (Nozue et al., 2007). The analysis of leaf growth in the wild type and *pif* mutants suggests that in leaves light does not shape growth rhythms primarily by controlling PIF4 and PIF5 abundance. First, the leaf growth peak occurs several hours after dawn, which is not consistent with light-induced degradation of growth promoting PIFs explaining this pattern (Figure 5). Second, in leaves the *pif4pif5* mutant maintains a growth rhythm similar to the wild type but with a reduced amplitude (Figure 7). Third, PIF4 over-expressing plants and *phyB* mutants which show reduced PIF4 degradation (de Lucas et al., 2008) maintain leaf growth rhythms with a robust amplitude in contrast to hypocotyls where this leads to dampened growth rhythms (Supplemental Figure 7) (Nozue et al., 2007). Our night extension and day-length experiments suggest that the light control of leaf growth has a strong metabolic component (Figures 5, 6, Supplemental Figure 5, 6). However, leaf growth patterns in constant light and reduced growth in *pif4pif5* clearly show the importance of PIF4, PIF5 and the circadian clock in regulating this process (Figures 5, 7, Supplemental Figure 7). Thus rhythmic leaf and hypocotyl growth are controlled by distinct mechanisms with a different role of light in shaping growth rhythms in both organs. It will be interesting to further contrast these growth rhythms in young leaves that largely rely on their own resources with those of roots or hypocotyls that depend on photosynthates exported from the leaves.

Finally, we would like to briefly speculate on the biological significance of diel rhythms of leaf growth rates and movements. A maximal peak of growth during the first few hours of the day matches with favorable conditions in terms of energetic requirements, water availability and auxin responsiveness (Covington and Harmer, 2007; Nozue et al., 2007; Stitt and Zeeman, 2012). Availability of resources also explains why more growth is observed at night in short-day-grown plants than in long-day-grown plants and the larger growth peak at dawn when Arabidopsis is grown in long days (Figure 5, Supplemental Figure 6) (Sulpice et al., 2013). The temperature cycles that accompany day-night transitions also contribute to the growth pattern (Sidaway-Lee et al., 2010; Bours et al., 2013). We note that the maximal growth rate identified in our conditions corresponds to the early morning when temperature is typically relatively low (Figure 5). Interestingly leaf elevation follows the typical daily temperature fluctuations with a peak in the late afternoon. Elevating leaves with this pattern is favorable to cool leaves during the warm hours of the day and diminishes the radiation load at times when it anyway surpasses photosynthetic capacity (Bridge et al., 2013).

Methods

Plant material and growth conditions

The *Arabidopsis thaliana* ecotype Col-0, the *pif4pif5* mutant (Nozue et al., 2007) and the *elf3-1* mutant (Liu et al., 2001) were grown on soil saturated with deionized water in a Percival CU-36L4 incubator (Percival Scientific, Inc., Perry, USA) at *T*=21°C, *R*H=85% relative humidity and *E*PAR=180 µmol m-2 s-1 for 13 days at long day (16/8h) or 17 days at short day (8/16h). Plants were transferred to the ScanAlyzer HTS (Lemnatec GmbH, Aachen, Germany) 24h before scanning for adaptation maintaining the growth conditions in the incubator. The light intensity in the measurement chamber was E_{PAR}=165 µmol m^{-2} s^{-1} and reduced to E_{PAR}=35 µmol m^{-2} s^{-1} for the low PAR treatment. The red/far-red ratio (R/FR) was decreased from R/FR = 5.59 to R/FR=0.49 using FR-emitting diodes. Further experimental details, spectral composition of light, computation of R/FR ratio and technical specification of the phenotyping device are described in more detail by (Dornbusch et al., 2012) and are available on our website (http://plantgrowth.vital-it.ch).

Analysis of leaf growth rates and elevation angles

A detailed description of the geometric definition of leaf length and elevation angle, image and data processing is presented in the supplemental information.

Supplemental Data

Supplemental Figure 1. Image analysis algorithm to compute P_P and P_T from time-lapse images.

Supplemental Figure 2. Definition of measured traits and principal output.

Supplemental Figure 3. In response to a low R/FR treatment the blade upward movement precedes the petiole upward movement.

Supplemental Figure 4. In L/D conditions the blade upward movement precedes the petiole upward movement.

Supplemental Figure 5: Light is required at dawn to trigger leaf growth.

Supplemental Figure 6. Growth and movements are altered by shortening day length or in continuous darkness.

Supplemental Figure 7: Plants with elevated levels of PIF4 maintain robust amplitude leaf growth rhythms.

Supplemental Movie 1 online. Semi-automated leaf-tracking on time-lapse 3D images of growing Arabidopsis plant

Supplemental Movie 2 online. Comparing leaf tracking on 3D images with manual leaf-selection on simultaneously photographed growing Arabidopsis plant.

Acknowledgements

This project was funded by grants from the Swiss SystemX.ch project (‘SyBIT’ to I. X. and ‘Plant Growth in a Changing Environment’ to I.X. and C. F.) and the University of Lausanne. T. D. benefitted from a Marie Curie Intra-European Fellowships (No. 275999). We thank the Department of Molecular Plant Biology of UNIL for the access to their plant facilities. We thank Seth Davis for providing *elf3-1* seeds, Mieke de Wit, Tobias Preuten and Samuel Zeeman (ETH, Zürich) for comments on the manuscript.

Author contribution

T. D. Designed research, contributed new analytic computational tools, performed research, analyzed data and wrote the article.
O. M. Designed research, contributed new analytic computational tools, performed research, analyzed data.
I. X. Contributed new analytic computational tools.
C.F. Designed research, analyzed data and wrote the article.

References

Andriankaja, M., Dhondt, S., De Bodt, S., Vanhaeren, H., Coppens, F., De Milde, L., Muhlenbock, P., Skirycz, A., Gonzalez, N., Beemster, G.T., and Inze, D. (2012). Exit from proliferation during leaf development in Arabidopsis thaliana: a not-so-gradual process. Dev Cell **22,** 64-78.

Barillot, R., Frak, E., Combes, D., Durand, J.L., and Escobar-Gutierrez, A.J. (2010). What determines the complex kinetics of stomatal conductance under blueless PAR in Festuca arundinacea? Subsequent effects on leaf transpiration. J Exp Bot **61,** 2795-2806.

Bours, R., Muthuraman, M., Bouwmeester, H., and van der Krol, A. (2012). OSCILLATOR: A system for analysis of diurnal leaf growth using infrared photography combined with wavelet transformation. Plant Methods **8,** 29.

Bours, R., van Zanten, M., Pierik, R., Bouwmeester, H., and van der Krol, A. (2013). Antiphase Light and Temperature Cycles Affect PHYTOCHROME B-Controlled Ethylene Sensitivity and Biosynthesis, Limiting Leaf Movement and Growth of Arabidopsis. Plant Physiol **163,** 882-895.

Bridge, L.J., Franklin, K.A., and Homer, M.E. (2013). Impact of plant shoot architecture on leaf cooling: a coupled heat and mass transfer model. J R Soc Interface **10,** 20130326.

Covington, M.F., and Harmer, S.L. (2007). The circadian clock regulates auxin signaling and responses in Arabidopsis. Plos Biol **5,** 1773-1784.

de Lucas, M., Daviere, J.M., Rodriguez-Falcon, M., Pontin, M., Iglesias-Pedraz, J.M., Lorrain, S., Fankhauser, C., Blazquez, M.A., Titarenko, E., and Prat, S. (2008). A molecular framework for light and gibberellin control of cell elongation. Nature **451,** 480-484.

Dornbusch, T., Lorrain, S., Kuznetsov, D., Fortier, A., Liechti, R., Xenarios, I., and Fankhauser, C. (2012). Measuring the diurnal pattern of leaf hyponasty and growth in Arabidopsis - a novel phenotyping approach using laser scanning. Funct Plant Biol **39,** 860-869.

Farre, E.M. (2012). The regulation of plant growth by the circadian clock. Plant Biol (Stuttg) **14,** 401-410.

Graf, A., Schlereth, A., Stitt, M., and Smith, A.M. (2010). Circadian control of carbohydrate availability for growth in Arabidopsis plants at night. Proc Natl Acad Sci U S A **107,** 9458-9463.

Ichihashi, Y., Kawade, K., Usami, T., Horiguchi, G., Takahashi, T., and Tsukaya, H. (2011). Key Proliferative Activity in the Junction between the Leaf Blade and Leaf Petiole of Arabidopsis. Plant Physiology **157,** 1151-1162.

Izumi, M., Hidema, J., Makino, A., and Ishida, H. (2013). Autophagy Contributes to Nighttime Energy Availability for Growth in Arabidopsis. Plant Physiology **161,** 1682-1693.

Keller, M.M., Jaillais, Y., Pedmale, U.V., Moreno, J.E., Chory, J., and Ballare, C.L. (2011). Cryptochrome 1 and phytochrome B control shade-avoidance responses in Arabidopsis via partially independent hormonal cascades. Plant J **67,** 195-207.

Lilley, J.L.S., Gee, C.W., Sairanen, I., Ljung, K., and Nemhauser, J.L. (2012). An Endogenous Carbon-Sensing Pathway Triggers Increased Auxin Flux and Hypocotyl Elongation. Plant Physiology **160,** 2261-2270.

Liu, X.L., Covington, M.F., Fankhauser, C., Chory, J., and Wagner, D.R. (2001). ELF3 encodes a circadian clock-regulated nuclear protein that functions in an Arabidopsis PHYB signal transduction pathway. Plant Cell **13,** 1293-1304.

Moreno, J.E., Tao, Y., Chory, J., and Ballare, C.L. (2009). Ecological modulation of plant defense via phytochrome control of jasmonate sensitivity. Proc Natl Acad Sci U S A **106,** 4935-4940.

Mullen, J.L., Weinig, C., and Hangarter, R.P. (2006). Shade avoidance and the regulation of leaf inclination in Arabidopsis. Plant Cell Environ **29,** 1099-1106.

Nozue, K., Covington, M.F., Duek, P.D., Lorrain, S., Fankhauser, C., Harmer, S.L., and Maloof, J.N. (2007). Rhythmic growth explained by coincidence between internal and external cues. Nature **448,** 358-361.

Nusinow, D.A., Helfer, A., Hamilton, E.E., King, J.J., Imaizumi, T., Schultz, T.F., Farre, E.M., and Kay, S.A. (2011). The ELF4-ELF3-LUX complex links the circadian clock to diurnal control of hypocotyl growth. Nature **475,** 398-402.

Paparelli, E., Parlanti, S., Gonzali, S., Novi, G., Mariotti, L., Ceccarelli, N., van Dongen, J.T., Kolling, K., Zeeman, S.C., and Perata, P. (2013). Nighttime Sugar Starvation Orchestrates Gibberellin Biosynthesis and Plant Growth in Arabidopsis. Plant Cell.

Polko, J.K., van Zanten, M., van Rooij, J.A., Maree, A.F., Voesenek, L.A., Peeters, A.J., and Pierik, R. (2012). Ethylene-induced differential petiole growth in Arabidopsis thaliana involves local microtubule reorientation and cell expansion. New Phytol **193,** 339-348.

Rauf, M., Arif, M., Fisahn, J., Xue, G.P., Balazadeh, S., and Mueller-Roeber, B. (2013). NAC transcription factor speedy hyponastic growth regulates flooding-induced leaf movement in Arabidopsis. Plant Cell **25,** 4941-4955.

Remmler, L., and Rolland-Lagan, A.G. (2012). Computational method for quantifying growth patterns at the adaxial leaf surface in three dimensions. Plant Physiol **159,** 27-39.

Ruts, T., Matsubara, S., Wiese-Klinkenberg, A., and Walter, A. (2012a). Diel patterns of leaf and root growth: endogenous rhythmicity or environmental response? J Exp Bot **63,** 3339-3351.

Ruts, T., Matsubara, S., Wiese-Klinkenberg, A., and Walter, A. (2012b). Aberrant temporal growth pattern and morphology of root and shoot caused by a defective circadian clock in Arabidopsis thaliana. Plant J **72,** 154-161.

Sidaway-Lee, K., Josse, E.M., Brown, A., Gan, Y., Halliday, K.J., Graham, I.A., and Penfield, S. (2010). SPATULA links daytime temperature and plant growth rate. Curr Biol **20,** 1493-1497.

Stewart, J.L., Maloof, J.N., and Nemhauser, J.L. (2011). PIF genes mediate the effect of sucrose on seedling growth dynamics. PLoS One **6,** e19894.

Stitt, M., and Zeeman, S.C. (2012). Starch turnover: pathways, regulation and role in growth. Curr Opin Plant Biol **15,** 282-292.

Stolarz, M. (2009). Circumnutation as a visible plant action and reaction: physiological, cellular and molecular basis for circumnutations. Plant Signal Behav **4,** 380-387.

Sulpice, R., Flis, A., Ivakov, A.A., Apelt, F., Krohn, N., Encke, B., Abel, C., Feil, R., Lunn, J.E., and Stitt, M. (2013). Arabidopsis Coordinates the Diurnal Regulation of Carbon Allocation and Growth across a Wide Range of Photoperiods. Mol Plant.

Suttangkakul, A., Li, F.Q., Chung, T., and Vierstra, R.D. (2011). The ATG1/ATG13 Protein Kinase Complex Is Both a Regulator and a Target of Autophagic Recycling in Arabidopsis. Plant Cell **23,** 3761-3779.

Tao, Y., Ferrer, J.L., Ljung, K., Pojer, F., Hong, F., Long, J.A., Li, L., Moreno, J.E., Bowman, M.E., Ivans, L.J., Cheng, Y., Lim, J., Zhao, Y., Ballare, C.L., Sandberg, G., Noel, J.P., and Chory, J. (2008). Rapid synthesis of auxin via a new tryptophan-dependent pathway is required for shade avoidance in plants. Cell **133,** 164-176.

Usadel, B., Blasing, O.E., Gibon, Y., Retzlaff, K., Hoehne, M., Gunther, M., and Stitt, M. (2008). Global transcript levels respond to small changes of the carbon status during progressive exhaustion of carbohydrates in Arabidopsis rosettes. Plant Physiology **146,** 1834-1861.

Walter, A., Silk, W.K., and Schurr, U. (2009). Environmental effects on spatial and temporal patterns of leaf and root growth. Annu Rev Plant Biol **60,** 279-304.

Whippo, C.W., and Hangarter, R.P. (2009). The "sensational" power of movement in plants: A Darwinian system for studying the evolution of behavior. Am J Bot **96,** 2115-2127.

Wiese, A., Christ, M.M., Virnich, O., Schurr, U., and Walter, A. (2007). Spatio-temporal leaf growth patterns of Arabidopsis thaliana and evidence for sugar control of the diel leaf growth cycle. New Phytol **174,** 752-761.

Yazdanbakhsh, N., Sulpice, R., Graf, A., Stitt, M., and Fisahn, J. (2011). Circadian control of root elongation and C partitioning in Arabidopsis thaliana. Plant Cell Environ **34,** 877-894.

Figure legends

Figure 1. Development and validation of a method for live measurements of leaf growth and leaf movements.

(A) Silhouette image taken with an infra-red sensitive camera from the side and top-down (indent); three characteristic points define dimension and orientation of each leaf and were manually selected: P_0 –shoot apical meristem, P_P –blade-petiole junction and P_T –leaf tip.

(B) The laser scanner renders the plant surface as 3D point cloud. The points P_0, P_P and P_T are computed for each leaf using a semi-automated image analysis algorithm. We simultaneously photographed and scanned 27 individual leaves over 48 h and compared values for P_0, P_P and P_T determined with each method.

(C) Length of petiole (brown dots) and leaf length (green dots) measured from silhouette images (x-axis) plotted against corresponding values computed with our algorithm (y-axis).

(D) Petiole elevation angle (blue dots) and leaf elevation angle (orange dots) measured from silhouette images (x-axis) plotted against corresponding values computed with our algorithm (y-axis). Solid black line is the 1:1 line, n = number of data points, R^2 = coefficient of determination, MAE = mean absolute error.

Figure 2: The pattern of leaf growth and movements in constant light.

(A) Leaf elongation rate, **(B)** leaf elevation angle and **(C)** leaf movements (angular rate of change) of leaf 1, 2 in continuous day (L/L; n_{leaf}=43). Curves highlighted in red represent phases of upward and curves in blue phases of downward movement. Col-0 plants were grown for 14 days in L/D conditions and imaged in L/L. Vertical gray bars represent subjective night periods. Leaf elongation rate is computed as mean moving average (3h) of individual curves. Leaf elevation angle and movement rates are mean values. The opaque band around the mean lines is the 95% confidence interval of mean estimate and n_{leaf} = number of leaves.

Figure 3: Blade and petiole movements contribute to the leaf hyponastic response.

(A) Leaf elongation rate and leaf movements (angular rate of change) of leaf 1, 2 in continuous day were replotted from Figure 2A and 2C for better direct comparison **(B)** Leaf elongation rate, **(C)** leaf elevation angle and **(D)** leaf movements (angular rate of change) of petioles (in red) and blades (in blue) of leaf 1, 2 in continuous day (L/L; n_{leaf}=32). Col-0 plants were grown for 14 days in L/D conditions and imaged in L/L. Vertical gray bars represent subjective night periods. Leaf elongation rate is computed as mean moving average (3h) of individual curves. Leaf elevation angle and movement rates are mean values. The opaque band around the mean lines is the 95% confidence interval of mean estimate. Arrows indicate acceleration of growth, n_{leaf} = number of leaves.

Figure 4. The magnitude of growth and movements are differentially affected by decreasing light intensity and day length.

Diel leaf elongation rate and leaf movement of leaf 1,2 (24h period). Diel elongation rates and leaf movements (absolute changes in leaf elevation angle) were computed summing up hourly rates over a period of 24h starting from ZT2.25. Col-0 plants were grown for 14 days under long day (16/8h) and imaged for 24h in constant light (L/L; n_{leaf}=43), in day-night cycles (L/D, n_{leaf}=27), in low light intensity (low PAR; n_{leaf}=57) maintaining L/D (PAR=35 µmol m^{-2} s^{-1}) and in continuous darkness (D/D; n_{leaf}=41). For the short-day experiment Col-0 was grown for 18 days in S/D (8/16h) before imaging under the same conditions (n_{leaf}=47). n_{leaf} = number of leaves**.**

Figure 5. Day-night transitions alter rhythmic growth and movements. **(A)** Leaf elongation rate, **(B)** leaf elevation angle and **(C)** leaf movements (angular rate of change) of leaf 1, 2 in continuous day (L/L; blue line; n_{leaf}=43) and long day conditions (L/D; 16/8; black line, n_{leaf}=27); Col-0 plants were grown for 14 days in L/D conditions. Plants were imaged either in L/L or in L/D. Vertical gray bars represent subjective or true night periods. Leaf elongation rate is computed as mean moving average (3h) of individual curves. Leaf elevation angle and movement rates are mean values. The opaque band around the mean lines is the 95% confidence

interval of mean estimate. Arrows indicate acceleration of growth, n_{leaf} = number of leaves.

Figure 6: Light is required at dawn to trigger leaf growth.

(A) Leaf elongation rate of leaf 1, 2 in long day (L/D, black line, n_{leaf}=27) and in +3h prolonged night period after dawn (L/D_{+3}; red line n_{leaf}=27**), (B)** Leaf elongation rate in L/D (black line) and in +3h prolonged night period before dusk (L/+3D; blue line, n_{leaf}=54). Col-0 plants were grown for 14 days under L/D (16/8) conditions before measurement; vertical gray bars represent true night periods; vertical red/blue bars indicate prolonged night periods. Leaf elongation rate is computed as mean moving average (3h) of individual curves. The opaque band around the mean lines is the 95% confidence interval of mean estimate, n_{leaf} = number of leaves**.**

Figure 7: The role of PIF4, PIF5 and ELF3 in establishing rhythmic leaf growth and movement. Leaf elongation rate and leaf elevation angle of leaf 1, 2. Col-0, *elf*3-1 and *pif4pif5* plants were grown for 14 days in L/D conditions prior to imaging in the indicated conditions. Leaf elongation rate is computed as mean moving average (3h) of individual curves. Leaf elevation angle are mean values. Vertical gray bars represent subjective or true night periods. The opaque band around the mean lines is the 95% confidence interval of mean estimate. n_{leaf} = number of leaves.

(A) In the *pif4pif5* double mutant grown in long-day conditions n_{leaf}=48.

(B) In the clock mutant *elf3-1* in long-day conditions n_{leaf}=45. Note that in *elf3-1* the peak of elevation angle and maximal growth coincide (blue arrows) while in the WT there is a large phase shift (black arrows).

(C) In the *pif4pif5* double mutant grown in continuous light n_{leaf}=46.

(D) In the clock mutant *elf3-1* grown in continuous light n_{leaf}=23.

Figure 1

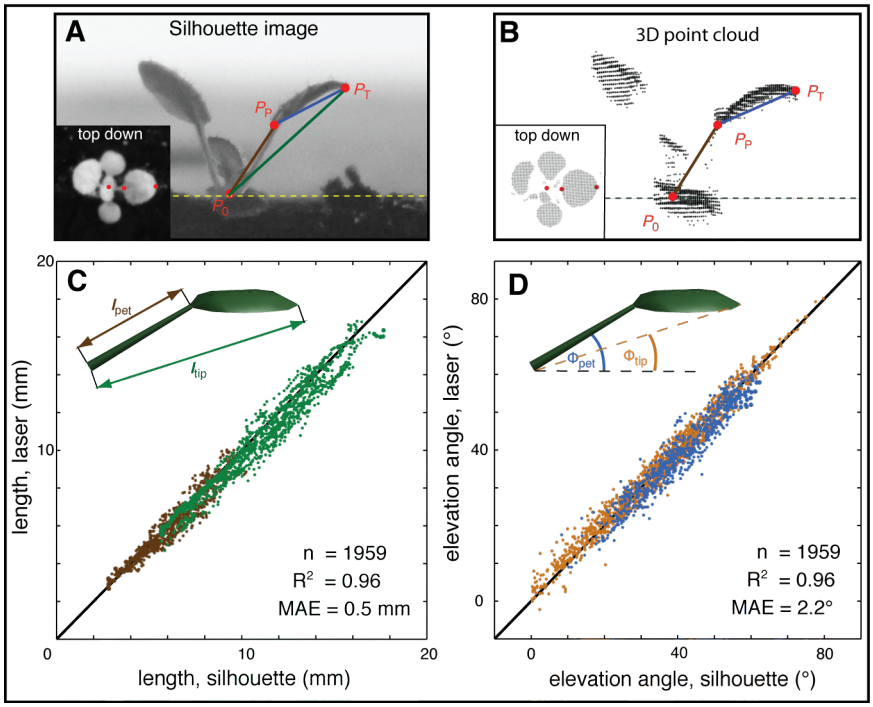

Figure 1. Development of a method for live measurements of leaf growth and leaf movements.

(A) Silhouette image taken with an infra-red sensitive camera from the side and top-down (indent); three characteristic points define dimension and orientation of each leaf and were manually selected: P_0 –shoot apical meristem, P_P –blade-petiole junction and P_T –leaf tip.

(B) The laser scanner renders the plant surface as 3D point cloud. The points P_0, P_P and P_T are computed for each leaf using a semi-automated image analysis algorithm. We simultaneously photographed and scanned 27 individual leaves over 48 h and compared values for P_0, P_P and P_T determined with each method.

(C) Length of petiole (brown dots) and leaf length (green dots) measured from silhouette images (x-axis) plotted against corresponding values computed with our algorithm (y-axis).

(D) Petiole elevation angle (blue dots) and leaf elevation angle (orange dots) measured from silhouette images (x-axis) plotted against corresponding values computed with our algorithm (y-axis). Solid black line is the 1:1 line, n = number of data points, R^2 = coefficient of determination, MAE = mean absolute error.

Figure 2

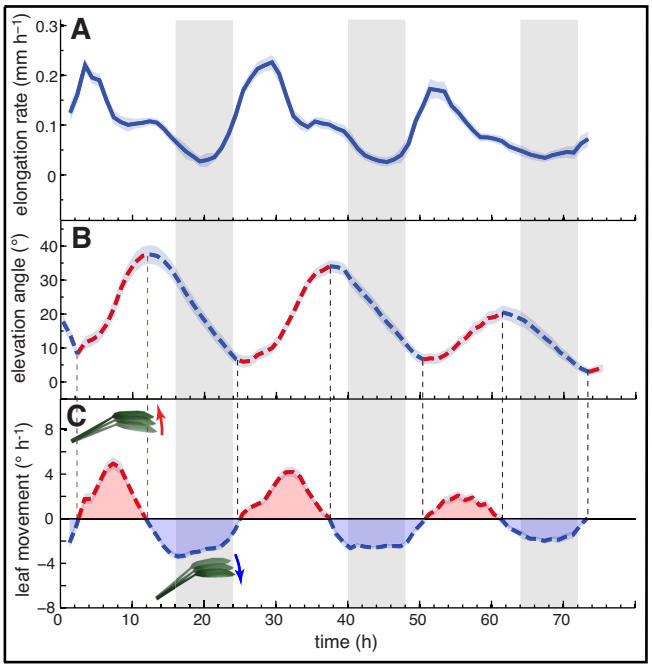

Figure 2: The pattern of leaf growth and movements in constant light.
(A) Leaf elongation rate, **(B)** leaf elevation angle and **(C)** leaf movements (angular rate of change) of leaf 1, 2 in continuous day (L/L; n_{leaf}=43). Curves highlighted in red represent phases of upward and curves in blue phases of downward movement. Col-0 plants were grown for 14 days in L/D conditions and imaged in L/L. Vertical gray bars represent subjective night periods. Leaf elongation rate is computed as mean moving average (3h) of individual curves. Leaf elevation angle and movement rates are mean values. The opaque band around the mean lines is the 95% confidence interval of mean estimate and n_{leaf} = number of leaves.

Figure 3

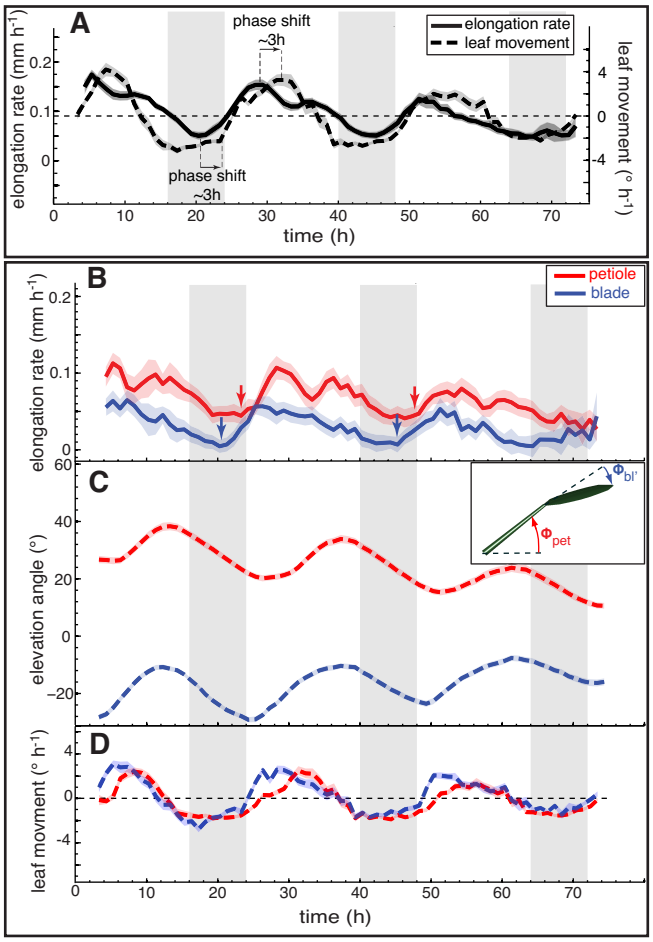

Figure 3: Blade and petiole movements contribute to the leaf hyponastic response.

(A) Leaf elongation rate and leaf movements (angular rate of change) of leaf 1, 2 in continuous day were replotted from Figure 2A and 2C for better direct comparison **(B)** Leaf elongation rate, **(C)** leaf elevation angle and **(D)** leaf movements (angular rate of change) of petioles (in red) and blades (in blue) of leaf 1, 2 in continuous day (L/L; n_{leaf}=32). Col-0 plants were grown for 14 days in L/D conditions and imaged in L/L. Vertical gray bars represent subjective night periods. Leaf elongation rate is computed as mean moving average (3h) of individual curves. Leaf elevation angle and movement rates are mean values. The opaque band around the mean lines is the 95% confidence interval of mean estimate. Arrows indicate acceleration of growth, n_{leaf} = number of leaves.

Figure 4

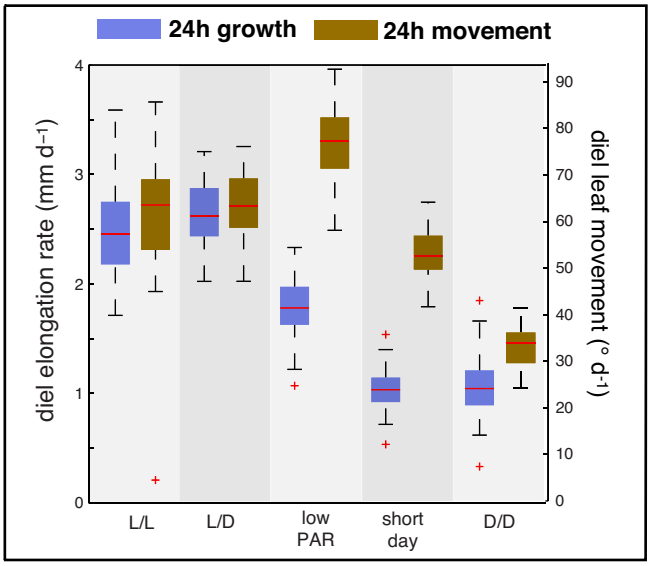

Figure 4. The magnitude of growth and movements are differentially affected by decreasing light intensity and day length.

Diel leaf elongation rate and leaf movement of leaf 1,2 (24h period). Diel elongation rates and leaf movements (absolute changes in leaf elevation angle) were computed summing up hourly rates over a period of 24h starting from ZT2.25. Col-0 plants were grown for 14 days under long day (16/8h) and imaged for 24h in constant light (L/L; n_{leaf}=43), in day-night cycles (L/D, n_{leaf}=27), in low light intensity (low PAR; n_{leaf}=57) maintaining L/D (PAR=35 µmol m^{-2} s^{-1}) and in continuous darkness (D/D; n_{leaf}=41). For the short-day experiment Col-0 was grown for 18 days in S/D (8/16h) before imaging under the same conditions (n_{leaf}=47). n_{leaf} = number of leaves**.**

Figure 5

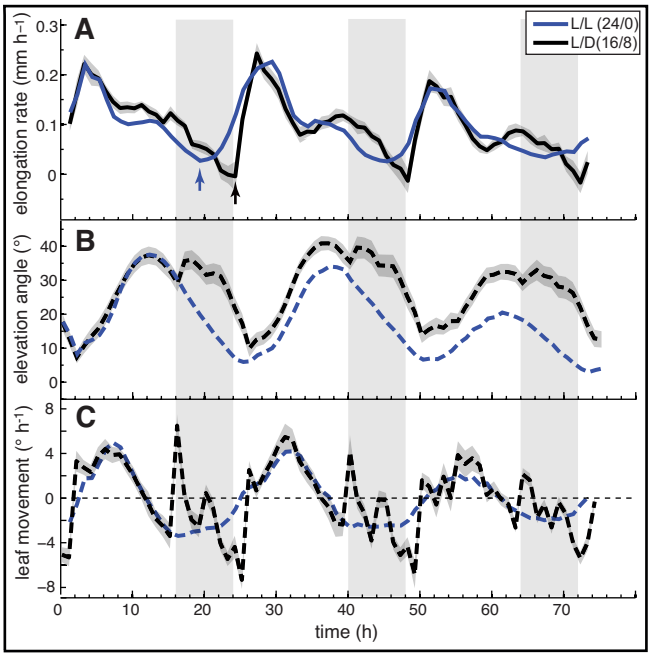

Figure 5. Day-night transitions alter rhythmic growth and movements. **(A)** Leaf elongation rate, **(B)** leaf elevation angle and **(C)** leaf movements (angular rate of change) of leaf 1, 2 in continuous day (L/L; blue line; n_{leaf}=43) and long day conditions (L/D; 16/8; black line, n_{leaf}=27); Col-0 plants were grown for 14 days in L/D conditions. Plants were imaged either in L/L or in L/D. Vertical gray bars represent subjective or true night periods. Leaf elongation rate is computed as mean moving average (3h) of individual curves. Leaf elevation angle and movement rates are mean values. The opaque band around the mean lines is the 95% confidence interval of mean estimate. Arrows indicate acceleration of growth, n_{leaf} = number of leaves.

Figure 6

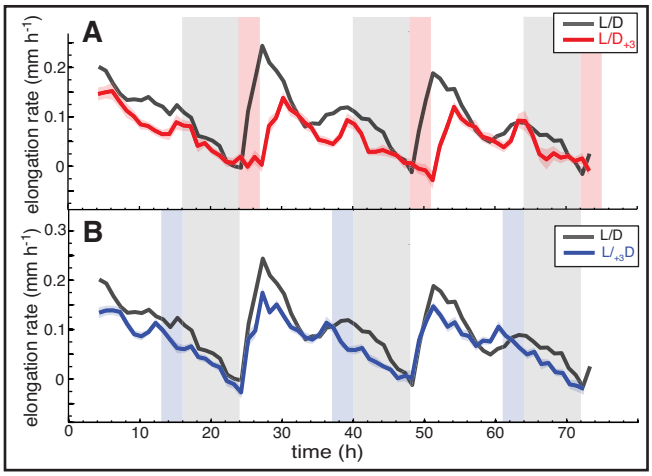

Figure 6: Light is required at dawn to trigger leaf growth.

(A) Leaf elongation rate of leaf 1, 2 in long day (L/D, black line, n_{leaf}=27) and in +3h prolonged night period after dawn (L/D_{+3}; red line n_{leaf}=27**), (B)** Leaf elongation rate in L/D (black line) and in +3h prolonged night period before dusk (L/+3D; blue line, n_{leaf}=54). Col-0 plants were grown for 14 days under L/D (16/8) conditions before measurement; vertical gray bars represent true night periods; vertical red/blue bars indicate prolonged night periods. Leaf elongation rate is computed as mean moving average (3h) of individual curves. The opaque band around the mean lines is the 95% confidence interval of mean estimate, n_{leaf} = number of leaves**.**

Figure 7

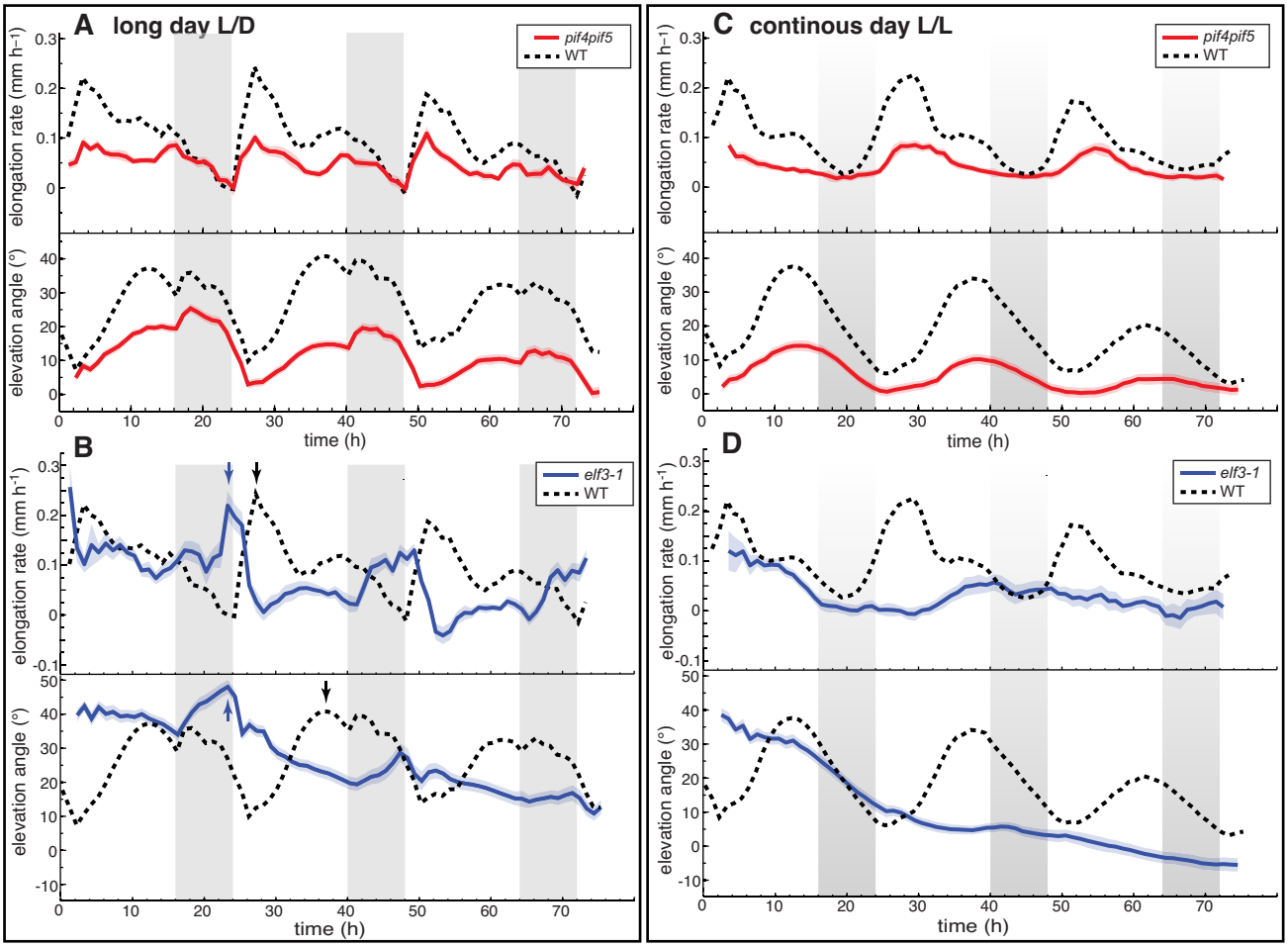

Figure 7: The role of PIF4, PIF5 and ELF3 in establishing rhythmic leaf growth and movement. Diurnal pattern of leaf elongation rate and leaf elevation angle of leaf 1, 2. Col-0, *elf*3-1 and *pif4pif5* plants were grown for 14 days in L/D conditions prior to imaging in the indicated conditions. Vertical gray bars represent subjective or true night periods. The opaque band around the mean lines is the 95% confidence interval of mean estimate. n_{leaf} = number of leaves.

(A) In the *pif4pif5* double mutant grown in long-day conditions n_{leaf}=48.

(B) In the clock mutant *elf3-1* in long-day conditions n_{leaf}=45. Note that in *elf3-1* the peak of elevation angle and maximal growth coincide (blue arrows) while in the WT there is a large phase shift (black arrows).

(C) In the *pif4pif5* double mutant grown in continuous light n_{leaf}=46.

(D) In the clock mutant *elf3-1* grown in continuous light n_{leaf}=23.

Figure S1

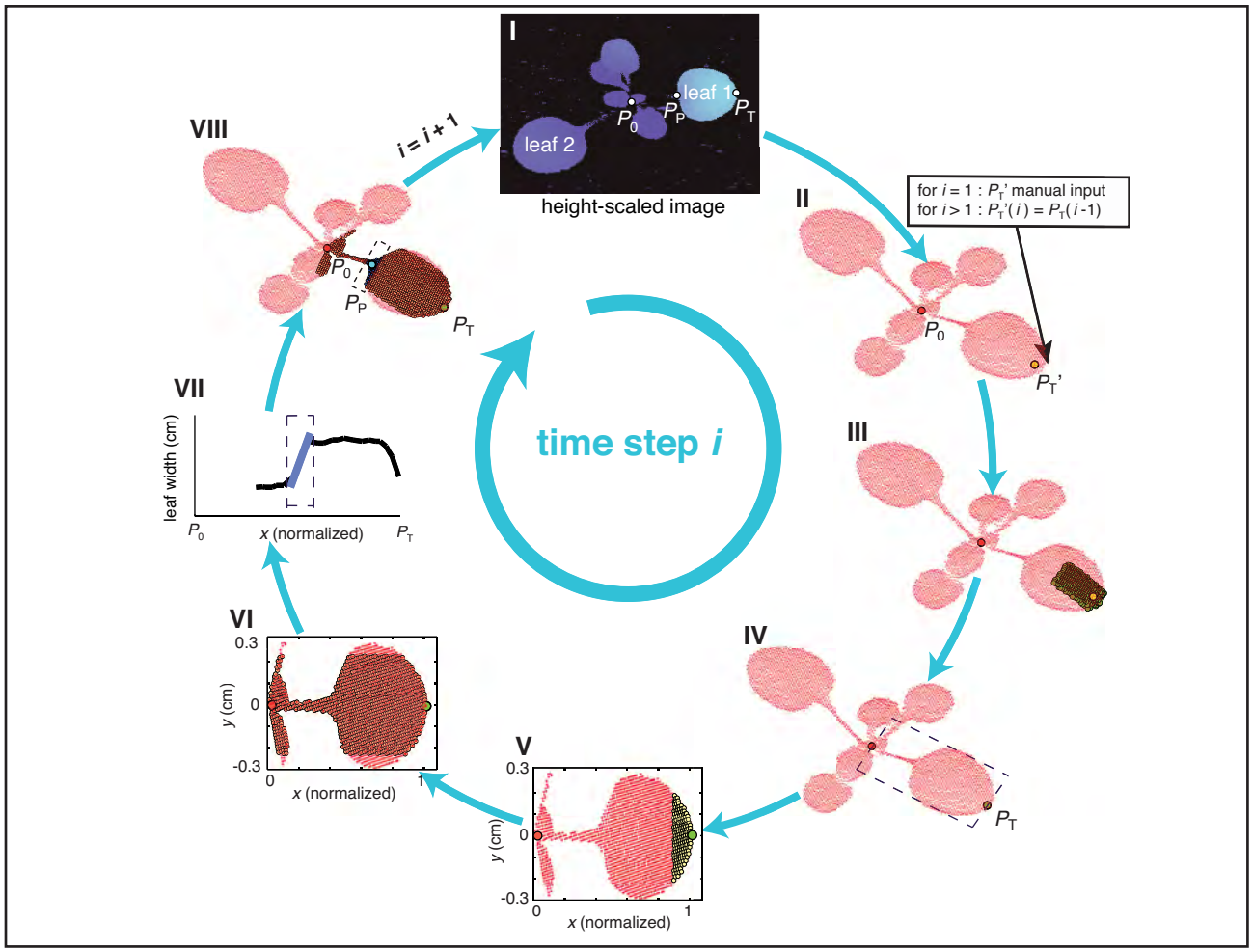

Supplemental Figure 1. Image analysis algorithm to compute P_P and P_T from time-lapse images.
Flow chart illustrating one time step *i* of the image analysis algorithm to compute the leaf tip point P_T and the petiole-blade intersection point P_P. I: Height-scaled image of a plant obtained with the laser scanner; II: point cloud representing the plant surface after 3D transformation; P_0 is manually selected each 24h at zeitgeber time (ZT) ZT3 or linearly interpolated for intermediate *i*; if *i*=1, the approximate leaf tip point $P_T'(1)$ is manually selected; if $i > 1$ the leaf tip point of the previous time step is used to enter the calculation: $P_T'(i) = P_T(i-1)$; III: filtering of points (in green) within a defined area around P_T'; IV: computation of P_T as the median of 10-20 leaf points with the largest distance to P_0; using P_0 and P_T, points are related to a leaf as highlighted by the dashed rectangle; V: selected points are rotated to the *x*-*y* plane and normalized such than $P_0 = (0,0,0)$ and $P_T = (0,1,0)$; approximated leaf width is computed using the highlighted points (in yellow) close to P_T; VI: highlighted points (in yellow) are filtered using the previously computed value for leaf width; VII: leaf width as a function of normalized axis position; the maximum of the first-order derivative is the approximate the position of P_P highlighted with a dashed rectangle; VIII: computation of P_P as is the centroid of selected points inside the dashed rectangle; in the subsequent iteration step *i*+1 the image of the same plant taken at the subsequent time step is processed and P_T and P_P computed for each leaf; the algorithm is automated and only needs user input at the first iteration step *i*=1.

Figure S2

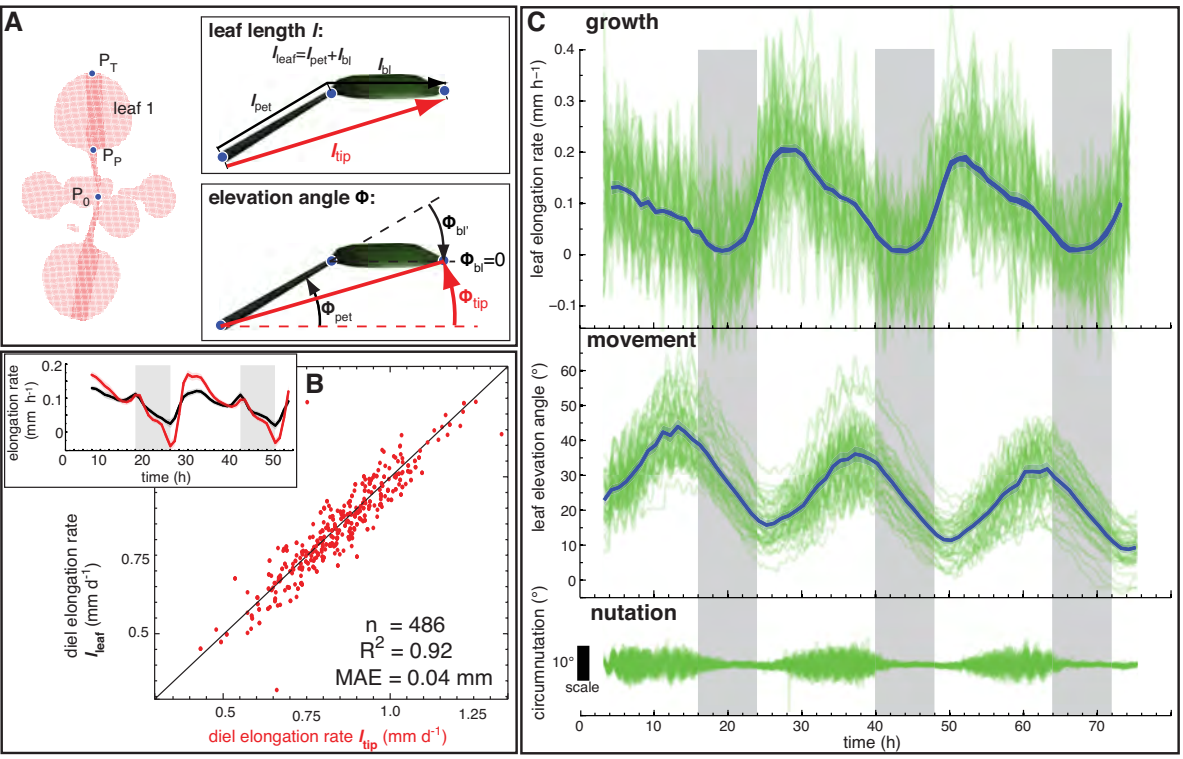

Supplemental Figure 2. Definition of measured traits and principal output.

(A) Geometric definition of leaf length and elevation angle. Arabidopsis plant as a measured 3D point cloud (red dots) viewed from top down (right). The points P_0 (position of meristem), P_P (position petiole-blade junction) and P_T (position of leaf tip) define length (l) and elevation angle (Φ) of the whole leaf (l_{tip}, Φ_{tip}), of the petiole (l_{pet}, Φ_{pet}) and of the blade (l_{bl}, Φ_{bl}) as illustrated in the indent figures.

(B) Comparison of diel (24h) elongation rate using l_{tip} and elongation rate using l_{leaf} of leaf 1 and 2. n = number of data points, R^2 = coefficient of determination, MAE = mean absolute error. Col-0 plants were grown for 14 days in long day (L/D, 16/8) conditions before measurement in L/D; the indent figure shows time courses of elongation rate as moving average over 3h using l_{leaf} (black line) and elongation rate using l_{tip} (red line); vertical gray bars represent true night periods. The colored opaque band (same color as mean line) is the 95% confidence interval of mean estimate.

(C) Leaf elongation rate, leaf elevation angle and circumnutations of leaf 1, 2 in continuous day (L/L). Col-0 plants were grown for 14 days in L/D (16/8) conditions before measurement in L/L; vertical gray bars represent subjective night periods. Opaque green lines represent data of 53 individual leaves. The solid blue line of leaf elongation rate is mean moving average (3h) of individual curves and the blue line of leaf elevation angle represent mean value of data points sampled each 60 min (conversely to individual data sampled each 10 min). The blue opaque band around the mean lines is the 95% confidence interval of mean estimate. Circumnutations are computed by detrending individual curves of leaf elevation angle using piecewise linear regression.

Figure S3

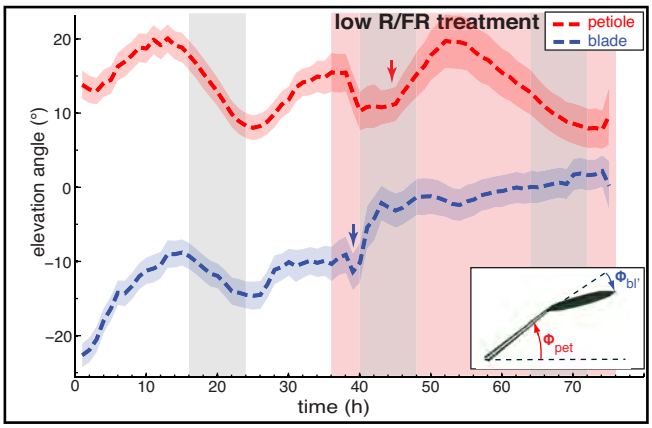

Supplemental Figure 3. In response to a low R/FR treatment the blade upward movement precedes the petiole upward movement.

Elevation angle of petioles (in red) and blades (in blue) of leaf 1, 2 in continuous day (n_{leaf}=28); Col-0 plants were grown for 14 days under long day (16/8) followed by 2 days continuous light (L/L) before measurement in L/L (subjective nights are darkened); after 36 hours the R/FR ratio was decreased to simulate shade (highlighted by the red rectangle). Leaf elevation angle are mean values. The opaque band around the mean lines is the 95% confidence interval of mean estimate. Arrows indicate the beginning of rapid upward movement, n_{leaf} = number of leaves.

Figure S4

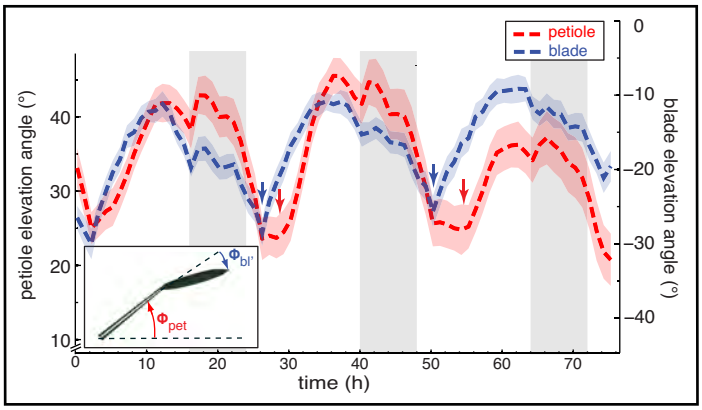

Supplemental Figure 4. In L/D conditions the blade upward movement precedes the petiole upward movement.

Elevation angle of petioles (in red; leaf scale) and blades (in blue, right scale) of leaf 1, 2 in long day conditions (L/D; 16/8; black line, n_{leaf}=19); Col-0 plants were grown for 14 days in L/D conditions and imaged at L/D. Vertical gray bars represent true night periods. Leaf elevation angle are mean values. The opaque band around the mean lines is the 95% confidence interval of mean estimate. Arrows indicate the beginning of rapid upward movement, n_{leaf} = number of leaves.

Figure S5

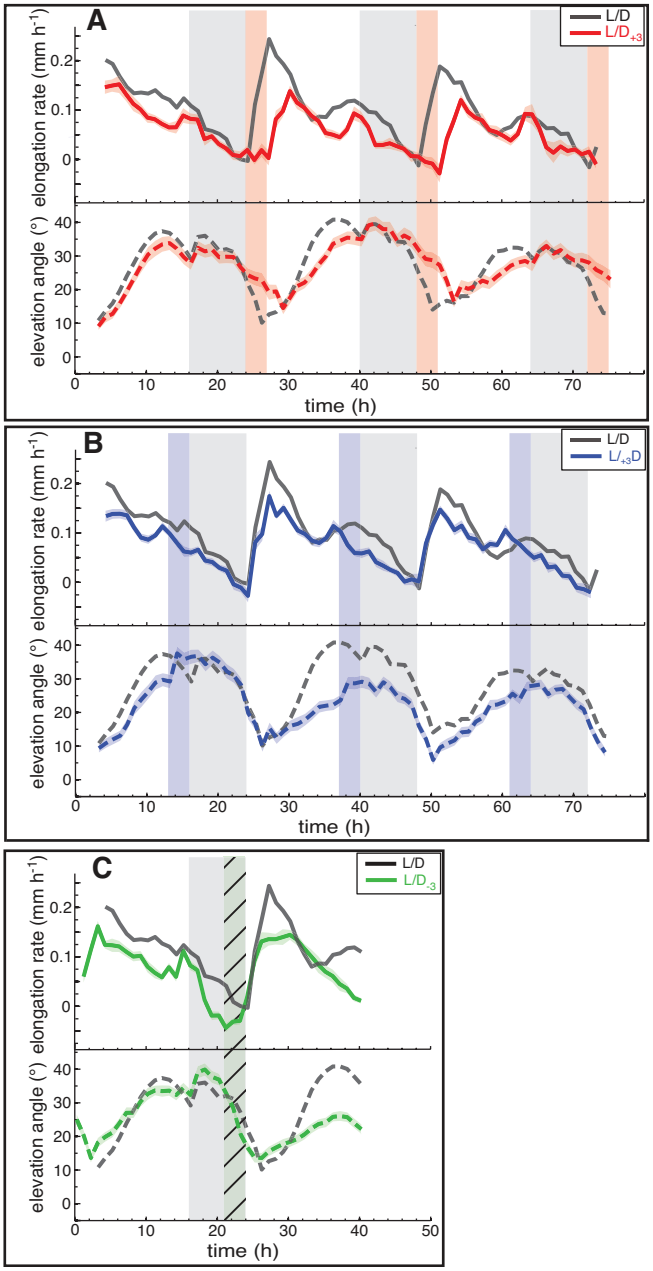

Supplemental Figure 5: Light is required at dawn to trigger leaf growth.

(A) This is the same growth data as plotted on Figure 6A, in addition we included leaf movement for those plants, night was prolonged after dawn by +3h (L/D_{+3}; red line n_{leaf}=27), **(B)** This is the same growth data as plotted on Figure 6B, in addition we included leaf movement for those plants, night was prolonged before dusk by +3h($L/_{+3}D$; blue line, n_{leaf}=54). **(C)** Leaf elongation rate and leaf elevation angle of leaf 1, 2 where night was shortened before dawn by -3h ($L/_{-3}D$; green line, n_{leaf}=60).

Col-0 plants were grown for 14 days under L/D (16/8) conditions before measurement; vertical gray bars represent true night periods; vertical red/blue bars indicate prolonged night periods (A,B) and vertical hatched green bar shortened night period (C). Solid lines of leaf elongation rate are the mean moving average (3h) of individual curves. Leaf elevation angle are mean values. The opaque band around the mean lines is the 95% confidence interval of mean estimate, n_{leaf} = number of leaves.

Figure S6

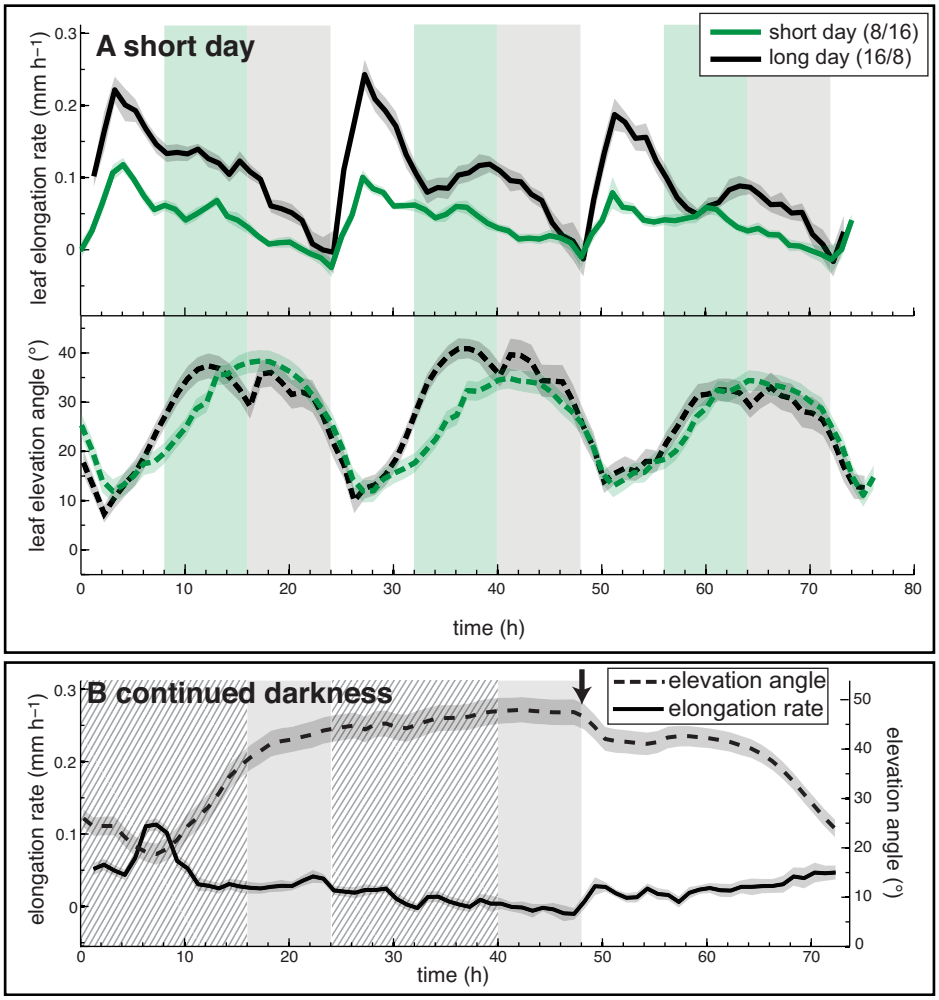

Supplemental Figure 6. Growth and movements are altered by shortening day length or in continuous darkness.

(A) Leaf elongation rate and leaf elevation angle of leaf 1, 2 in long day (black line, n_{leaf}=27) and short day (green line, n_{leaf}=47). Col-0 plants were grown for 14 days under long day (16/8h) or 18 days under short day (8/16h) condition before measurement under the same conditions

(B) Leaf elongation rate and leaf elevation angle of leaf 1, 2 in prolonged darkness (D/D, n_{leaf}=41). Col-0 plants were grown for 14 days under L/D (16/8) conditions before measurement and imaged in 48h of darkness followed by 24h of light; vertical gray bars represent subjective night periods and the hatched part the subjective day; The arrow marks the time when light was switched on. Solid lines of leaf elongation rate are the mean moving average (3h) of individual curves. Solid lines of leaf elevation angle are mean values. The opaque band around the mean lines is the 95% confidence interval of mean estimate. n_{leaf} = number of leaves.

Figure S7

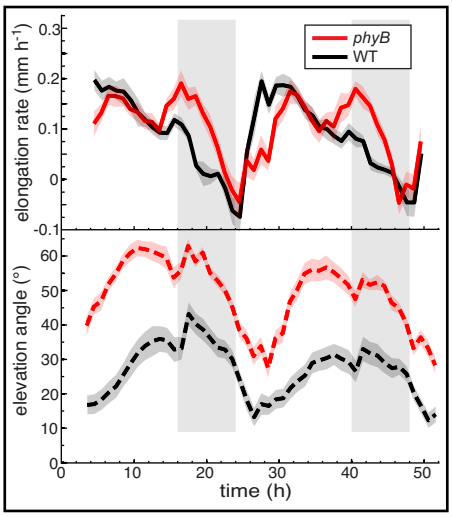

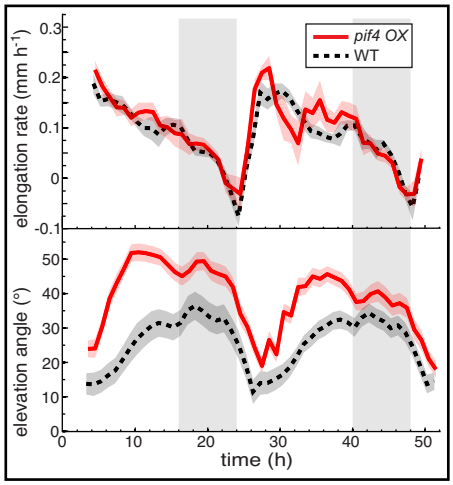

Supplemental Figure 7: Plants with elevated levels of PIF4 maintain robust amplitude leaf growth rhythms.

(A) Leaf elongation rate and leaf elevation angle of leaf 1, 2 in the *phyB* mutant (n_{leaf}=29) and Col-0 (n_{leaf}=30) grown in long-day conditions. **(B)** Leaf elongation rate and leaf elevation angle of leaf 1, 2 in the *PIF4 overexpressor* line (n_{leaf}=30) and Col-0 (n_{leaf}=30) grown in long-day conditions. Col-0, *phyB* and *PIF4 OX* plants were grown for 14 days in L/D conditions prior to imaging in the same conditions. Vertical gray bars representnight periods. Solid lines of leaf elongation rate are the mean moving average (3h) of individual curves. Leaf elevation angle are mean values. The opaque band around the mean lines is the 95% confidence interval of mean estimate. n_{leaf} = number of leaves.

Figure S1

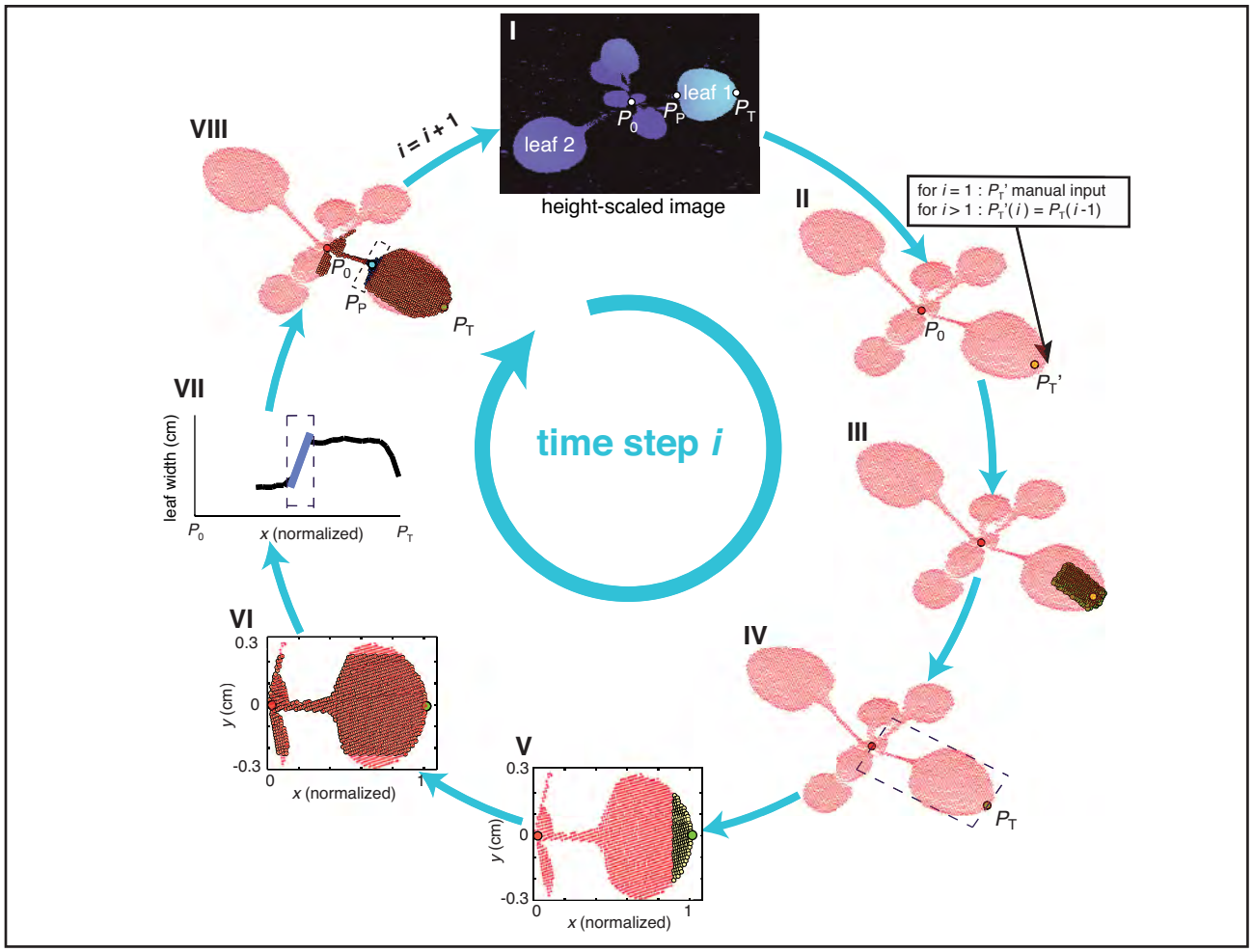

Supplemental Figure 1. Image analysis algorithm to compute P_P and P_T from time-lapse images.
Flow chart illustrating one time step *i* of the image analysis algorithm to compute the leaf tip point P_T and the petiole-blade intersection point P_P. I: Height-scaled image of a plant obtained with the laser scanner; II: point cloud representing the plant surface after 3D transformation; P_0 is manually selected each 24h at zeitgeber time (ZT) ZT3 or linearly interpolated for intermediate *i*; if *i*=1, the approximate leaf tip point $P_T'(1)$ is manually selected; if $i > 1$ the leaf tip point of the previous time step is used to enter the calculation: $P_T'(i) = P_T(i-1)$; III: filtering of points (in green) within a defined area around P_T'; IV: computation of P_T as the median of 10-20 leaf points with the largest distance to P_0; using P_0 and P_T, points are related to a leaf as highlighted by the dashed rectangle; V: selected points are rotated to the *x*-*y* plane and normalized such than $P_0 = (0,0,0)$ and $P_T = (0,1,0)$; approximated leaf width is computed using the highlighted points (in yellow) close to P_T; VI: highlighted points (in yellow) are filtered using the previously computed value for leaf width; VII: leaf width as a function of normalized axis position; the maximum of the first-order derivative is the approximate the position of P_P highlighted with a dashed rectangle; VIII: computation of P_P as is the centroid of selected points inside the dashed rectangle; in the subsequent iteration step *i*+1 the image of the same plant taken at the subsequent time step is processed and P_T and P_P computed for each leaf; the algorithm is automated and only needs user input at the first iteration step *i*=1.

Figure S2

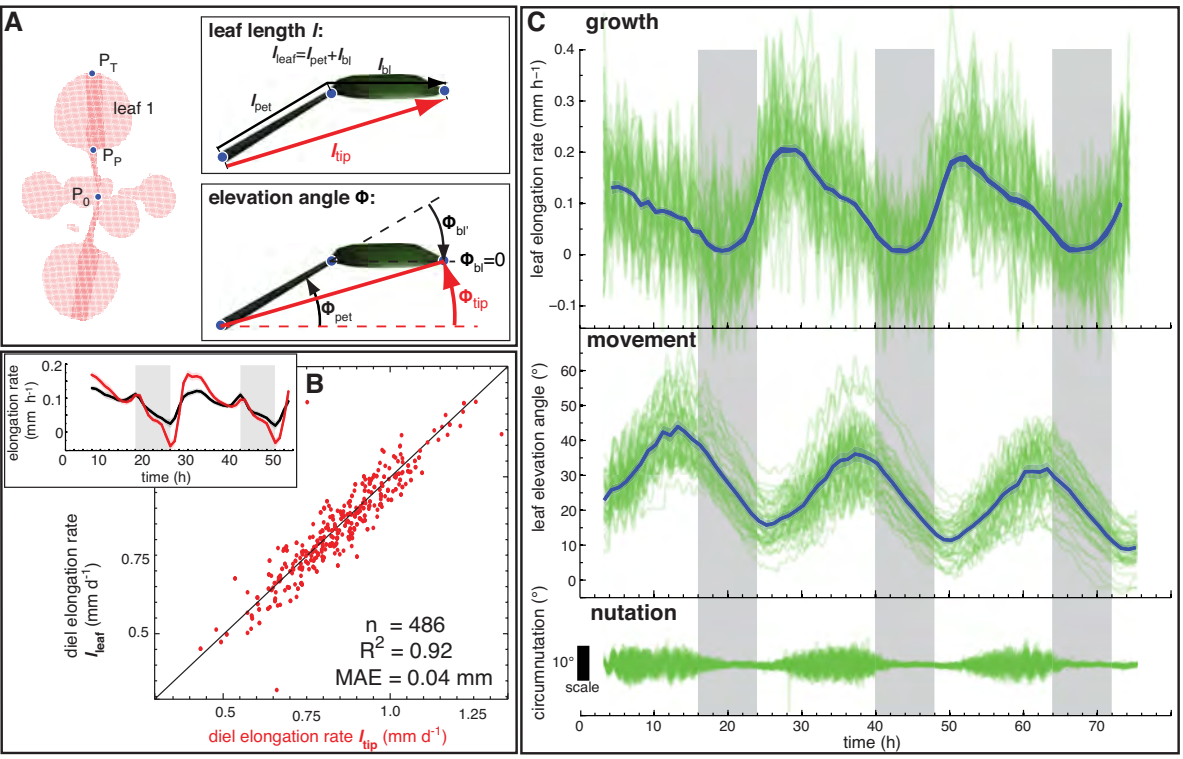

Supplemental Figure 2. Definition of measured traits and principal output.

(A) Geometric definition of leaf length and elevation angle. Arabidopsis plant as a measured 3D point cloud (red dots) viewed from top down (right). The points P_0 (position of meristem), P_P (position petiole-blade junction) and P_T (position of leaf tip) define length (l) and elevation angle (Φ) of the whole leaf (l_{tip}, Φ_{tip}), of the petiole (l_{pet}, Φ_{pet}) and of the blade (l_{bl}, Φ_{bl}) as illustrated in the indent figures.

(B) Comparison of diel (24h) elongation rate using l_{tip} and elongation rate using l_{leaf} of leaf 1 and 2. n = number of data points, R^2 = coefficient of determination, MAE = mean absolute error. Col-0 plants were grown for 14 days in long day (L/D, 16/8) conditions before measurement in L/D; the indent figure shows time courses of elongation rate as moving average over 3h using l_{leaf} (black line) and elongation rate using l_{tip} (red line); vertical gray bars represent true night periods. The colored opaque band (same color as mean line) is the 95% confidence interval of mean estimate.

(C) Leaf elongation rate, leaf elevation angle and circumnutations of leaf 1, 2 in continuous day (L/L). Col-0 plants were grown for 14 days in L/D (16/8) conditions before measurement in L/L; vertical gray bars represent subjective night periods. Opaque green lines represent data of 53 individual leaves. The solid blue line of leaf elongation rate is mean moving average (3h) of individual curves and the blue line of leaf elevation angle represent mean value of data points sampled each 60 min (conversely to individual data sampled each 10 min). The blue opaque band around the mean lines is the 95% confidence interval of mean estimate. Circumnutations are computed by detrending individual curves of leaf elevation angle using piecewise linear regression.

Figure S3

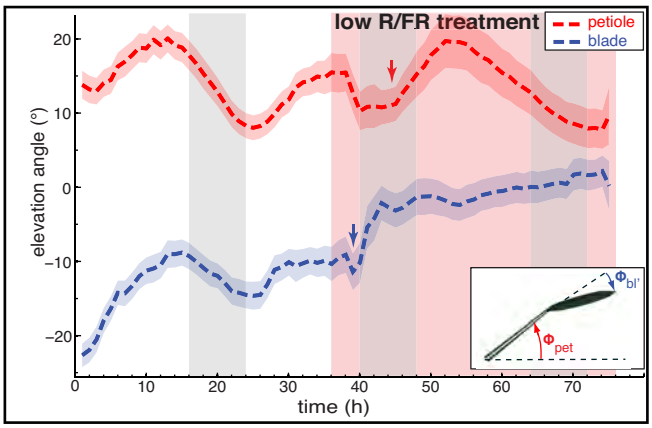

Supplemental Figure 3. In response to a low R/FR treatment the blade upward movement precedes the petiole upward movement.

Elevation angle of petioles (in red) and blades (in blue) of leaf 1, 2 in continuous day (n_{leaf}=28); Col-0 plants were grown for 14 days under long day (16/8) followed by 2 days continuous light (L/L) before measurement in L/L (subjective nights are darkened); after 36 hours the R/FR ratio was decreased to simulate shade (highlighted by the red rectangle). Leaf elevation angle are mean values. The opaque band around the mean lines is the 95% confidence interval of mean estimate. Arrows indicate the beginning of rapid upward movement, n_{leaf} = number of leaves.

Figure S4

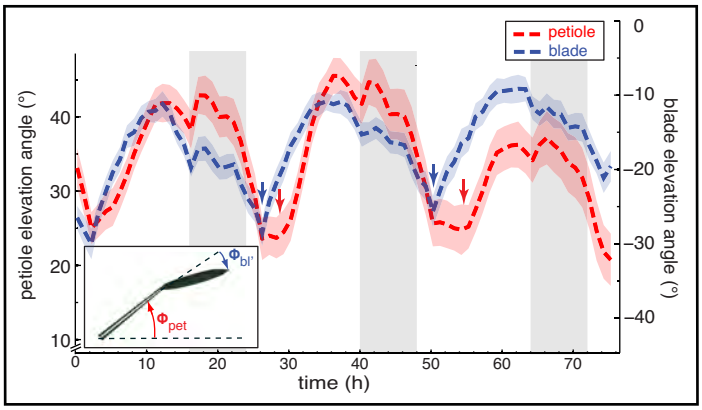

Supplemental Figure 4. In L/D conditions the blade upward movement precedes the petiole upward movement.

Elevation angle of petioles (in red; leaf scale) and blades (in blue, right scale) of leaf 1, 2 in long day conditions (L/D; 16/8; black line, n_{leaf}=19); Col-0 plants were grown for 14 days in L/D conditions and imaged at L/D. Vertical gray bars represent true night periods. Leaf elevation angle are mean values. The opaque band around the mean lines is the 95% confidence interval of mean estimate. Arrows indicate the beginning of rapid upward movement, n_{leaf} = number of leaves.

Figure S5

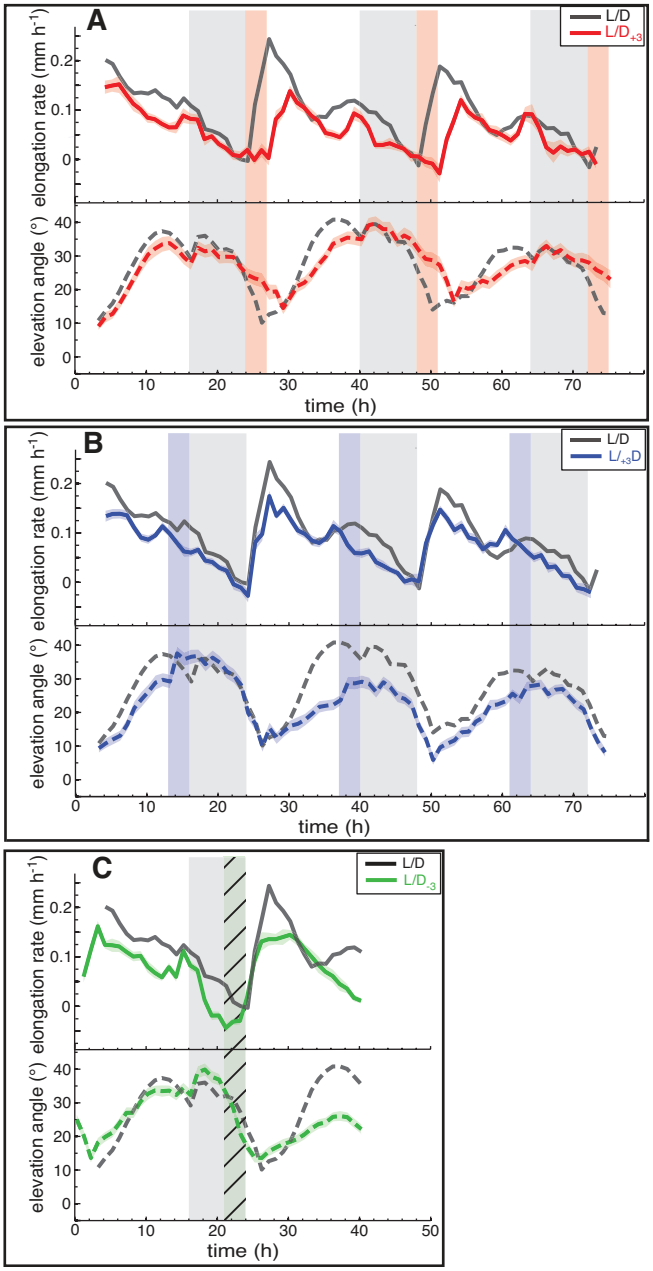

Supplemental Figure 5: Light is required at dawn to trigger leaf growth.

(A) This is the same growth data as plotted on Figure 6A, in addition we included leaf movement for those plants, night was prolonged after dawn by +3h (L/D_{+3}; red line n_{leaf}=27), **(B)** This is the same growth data as plotted on Figure 6B, in addition we included leaf movement for those plants, night was prolonged before dusk by +3h($L/_{+3}D$; blue line, n_{leaf}=54). **(C)** Leaf elongation rate and leaf elevation angle of leaf 1, 2 where night was shortened before dawn by -3h ($L/_{-3}D$; green line, n_{leaf}=60).

Col-0 plants were grown for 14 days under L/D (16/8) conditions before measurement; vertical gray bars represent true night periods; vertical red/blue bars indicate prolonged night periods (A,B) and vertical hatched green bar shortened night period (C). Solid lines of leaf elongation rate are the mean moving average (3h) of individual curves. Leaf elevation angle are mean values. The opaque band around the mean lines is the 95% confidence interval of mean estimate, n_{leaf} = number of leaves.

Figure S6

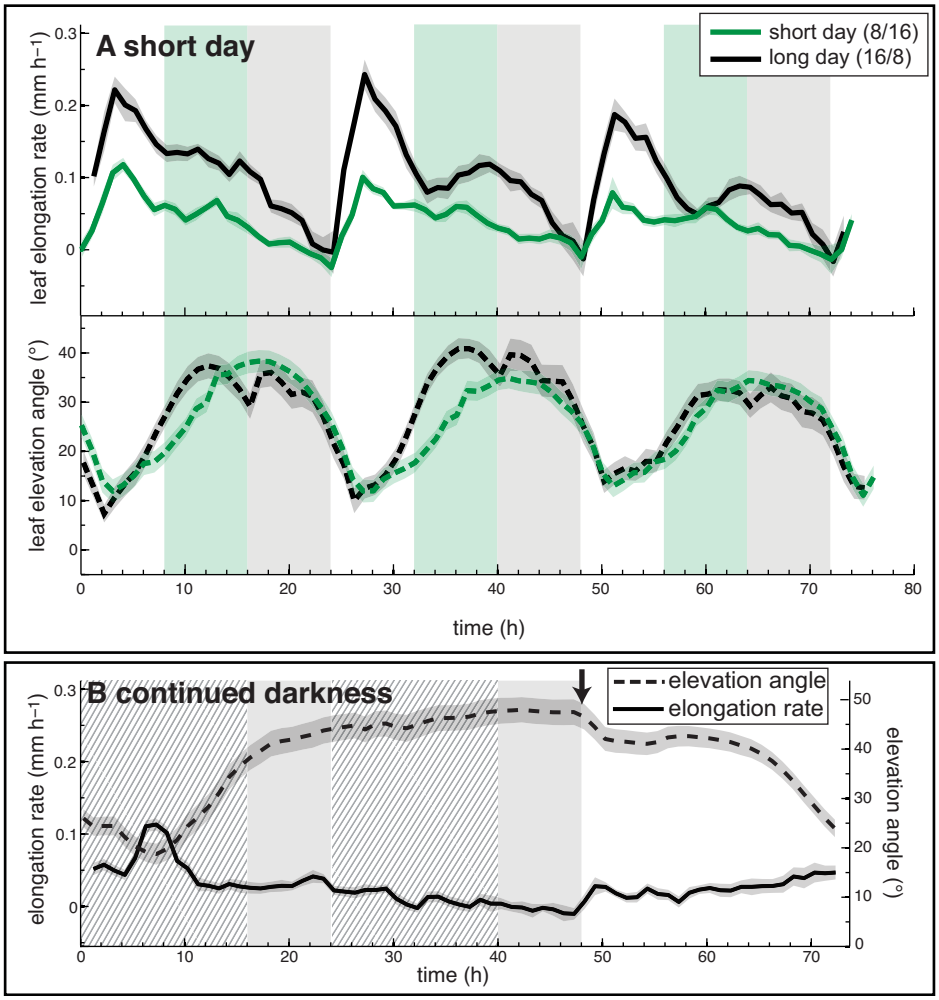

Supplemental Figure 6. Growth and movements are altered by shortening day length or in continuous darkness.

(A) Leaf elongation rate and leaf elevation angle of leaf 1, 2 in long day (black line, n_{leaf}=27) and short day (green line, n_{leaf}=47). Col-0 plants were grown for 14 days under long day (16/8h) or 18 days under short day (8/16h) condition before measurement under the same conditions

(B) Leaf elongation rate and leaf elevation angle of leaf 1, 2 in prolonged darkness (D/D, n_{leaf}=41). Col-0 plants were grown for 14 days under L/D (16/8) conditions before measurement and imaged in 48h of darkness followed by 24h of light; vertical gray bars represent subjective night periods and the hatched part the subjective day; The arrow marks the time when light was switched on. Solid lines of leaf elongation rate are the mean moving average (3h) of individual curves. Solid lines of leaf elevation angle are mean values. The opaque band around the mean lines is the 95% confidence interval of mean estimate. n_{leaf} = number of leaves.

Figure S7

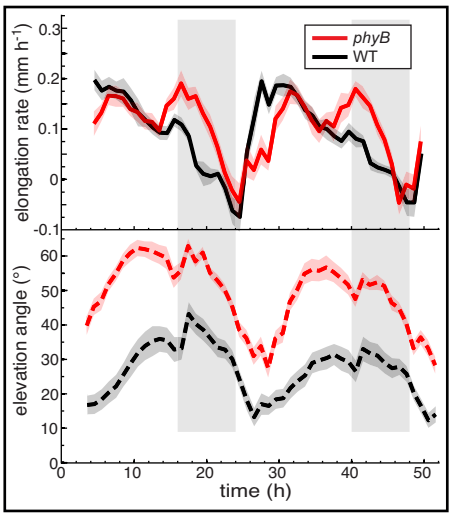

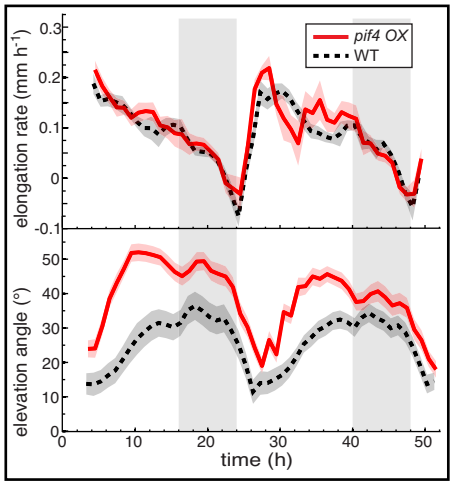

Supplemental Figure 7: Plants with elevated levels of PIF4 maintain robust amplitude leaf growth rhythms.

(A) Leaf elongation rate and leaf elevation angle of leaf 1, 2 in the *phyB* mutant (n_{leaf}=29) and Col-0 (n_{leaf}=30) grown in long-day conditions. **(B)** Leaf elongation rate and leaf elevation angle of leaf 1, 2 in the *PIF4 overexpressor* line (n_{leaf}=30) and Col-0 (n_{leaf}=30) grown in long-day conditions. Col-0, *phyB* and *PIF4 OX* plants were grown for 14 days in L/D conditions prior to imaging in the same conditions. Vertical gray bars representnight periods. Solid lines of leaf elongation rate are the mean moving average (3h) of individual curves. Leaf elevation angle are mean values. The opaque band around the mean lines is the 95% confidence interval of mean estimate. n_{leaf} = number of leaves.